The regulator LdhR and the D-lactate dehydrogenase LdhA of *Burkholderia multivorans* play a role in carbon overflow and in planktonic cellular aggregates formation

Running title: *Burkholderia multivorans* suspended biofilm

Inês N. Silva[1], Marcelo J. Ramires[1], Lisa A. Azevedo[1], Ana R. Guerreiro[1], Andreia C. Tavares[1*], Jörg D. Becker[2], and Leonilde M. Moreira[1,3#]

[1]IBB- Institute for Bioengineering and Biosciences, Instituto Superior Técnico (IST), Av. Rovisco Pais, 1049-001 Lisbon, Portugal

[2]Instituto Gulbenkian de Ciência, Rua da Quinta Grande Nº 6, 2780-156 Oeiras, Portugal

[3]Department of Bioengineering, IST, Universidade de Lisboa, Av. Rovisco Pais, 1049-001 Lisbon, Portugal

[#]Correspondence: Leonilde M. Moreira

Mailing address: Instituto Superior Técnico, Torre Sul, Piso 6, Av. Rovisco Pais, 1049-001 Lisbon, Portugal. Phone: (351)218419031. Fax: (351)218419199. E-mail: lmoreira@tecnico.ulisboa.pt

[*]Present address: Instituto de Tecnologia Química e Biológica António Xavier, ITQB NOVA, Avenida da República, 2780-157 Oeiras, Portugal

ABSTRACT

LysR-type transcriptional regulators (LTTR) are the most commonly found regulators in *Burkholderia cepacia* complex, comprising opportunistic pathogens causing chronic respiratory infections in cystic fibrosis (CF) patients. Despite LTTRs being global regulators of pathogenicity in several bacteria, few have been characterized in *Burkholderia*. Here, we showed that gene *ldhR* of *B. multivorans* encoding a LTTR is co-transcribed with *ldhA* encoding a D-lactate dehydrogenase, and evaluate their implication in virulence traits like exopolysaccharide (EPS) synthesis and biofilm formation. Comparison of wild-type (WT) and its isogenic Δ*ldhR* mutant grown in medium with 2% D-glucose revealed a negative impact on EPS biosynthesis and on cells´ viability in the presence of LdhR. Loss of viability in WT cells was caused by intracellular acidification as consequence of cumulative organic acids secretion including D-lactate, this last one absent from the Δ*ldhR* mutant supernatant. Furthermore, LdhR is implicated in the formation of planktonic cellular aggregates. WT cell aggregates reached 1000 μm after 24 hours in liquid cultures; in contrast to Δ*ldhR* mutant aggregates that never grew more than 60 μm. Overexpression of D-lactate dehydrogenase LdhA in the Δ*ldhR* mutant partially restored formed aggregates size, suggesting a role for fermentation inside aggregates. Similar results were obtained for surface-attached biofilms, with WT cells producing more biofilm. A systematic evaluation of planktonic aggregates in *Burkholderia* CF clinical isolates showed aggregates in 40 out of 74. As CF patients´ lung environment is microaerophilic and bacteria are found as free aggregates/biofilms, LdhR and LdhA might have central roles in adaptation to this environment.

47 **IMPORTANCE**

48 Cystic fibrosis patients often suffer from chronic respiratory infections caused by several
49 microorganisms. Among them are the *Burkholderia cepacia* complex bacteria which cause
50 progressive deterioration of lung function and, in some patients, might develop into fatal
51 necrotizing pneumoniae with bacteremia, known as “cepacia syndrome”. *Burkholderia*
52 pathogenesis is multifactorial since they express several virulence factors, form biofilms, and
53 are highly resistant to antimicrobial compounds, making their eradication from the CF patients´
54 airways very difficult. As *Burkholderia* is commonly found in the CF lungs in the form of cell
55 aggregates and biofilms, the need to investigate the mechanisms of cellular aggregation is
56 obvious. In this study we demonstrate the importance of a D-lactate dehydrogenase and a
57 regulator, in regulating carbon overflow, cellular aggregates and surface-attached biofilm
58 formation. This not only enhances our understanding of *Burkholderia* pathogenesis, but can
59 also lead to the development of drugs against these proteins to circumvent biofilm formation.
60

61 **Keywords:** LysR-family transcriptional regulator, D-lactate dehydrogenase, *Burkholderia*
62 *multivorans*, Planktonic cellular aggregates, Biofilms, Exopolysaccharide; Cystic fibrosis
63

INTRODUCTION

Burkholderia cepacia complex comprises bacteria ubiquitous in the environment, but also responsible for persistent infections in the airways of cystic fibrosis (CF) sufferers, strongly contributing to lung function deterioration (1). *Burkholderia* may grow as single cells, but they are often found in small clusters such as the ones identified in the airways of CF patients (2). To cope with the different environments, these bacteria are equipped with a wide range of metabolic functions and virulence traits, reflected in their genome size ranging from 6 to 9 Mbp (3, 4). One such trait shared by many *B. cepacia* complex strains is the expression of the mucoid phenotype due to the biosynthesis of exopolysaccharides (EPSs) (5, 6). One of those EPSs, cepacian, has been implicated in biofilm formation, inhibition of neutrophil chemotaxis, protection against phagocytosis by human neutrophils, neutralization of reactive oxygen species *in vitro*, facilitation of persistent bacterial infection in animal models, and protection against abiotic stressors (7–12). The synthesis in large amounts of this polymeric compound requires high carbon to nitrogen ratio, being mannitol or glucose commonly used carbon sources (6–8). One particular feature of glucose metabolism in *B. cepacia* complex bacteria is the presence of alternative routes for its conversion into gluconate-6P prior entry into the Entner-Doudoroff pathway: the direct oxidative pathway mediated by the activities of membrane-associated glucose and gluconate dehydrogenases, and the phosphorylative pathway mediated by glucokinase and a NAD(P)-dependent glucose 6P-dehydrogenase (Fig. 1) (13). The main utilization of one pathway or another is dependent on the glucose source and is strain specific (14). Whatever sugar is used as carbon source for EPS biosynthesis, it needs to be fed into the central metabolic pathways and the required activated sugar-nucleotide precursors

86 synthesized. Then, these sugar-nucleotide precursors are assembled into repeating units that are
87 subsequently polymerized and EPS chains secreted to the external milieu (5).

88 Although genes involved in cepacian biosynthesis have already been described (7, 15) the
89 regulation of transcription of those *bce*-I and *bce*-II gene clusters remains mostly unknown. To
90 understand the mechanisms regulating EPS production, Silva and coworkers compared the
91 transcriptome of mucoid and nonmucoid clonal isolates of *Burkholderia multivorans*, leading to
92 the identification of a putative LysR-type transcriptional regulator (LTTR) whose expression was
93 downregulated in the nonmucoid isolate (16). This LTTR is located upstream a gene encoding a
94 putative D-lactate dehydrogenase, an enzyme that reversibly converts pyruvate into D-lactate.
95 Besides the important role of D-lactate dehydrogenase in fermentation and energy production
96 under oxygen-limiting conditions, this metabolic conversion has been shown as required for
97 microcolony formation, a hallmark of biofilm architecture in *Pseudomonas aeruginosa* (17)
98 especially associated with CF lung infections (2, 18). Petrova and coworkers, by studying the
99 role of the two-component regulator MifR, demonstrated that inactivation of genes involved in
100 pyruvate utilization or depletion of pyruvate from the growth medium abrogated microcolony
101 formation, and pyruvate supplementation significantly increased microcolony formation (17).
102 Although that study revealed that MifR-dependent microcolony formation is associated with
103 stressful, oxygen-limiting yet electron-rich conditions, other mechanisms seem also to be
104 implicated in microcolony formation in *P. aeruginosa*. Indeed, the LTTR BvlR of *P. aeruginosa*
105 PA14 was implicated in tight microcolony formation possibly mediated through repression of
106 fimbrial-based surface attachment (19). Tight microcolonies (also named planktonic cellular
107 aggregates) are a mode of biofilm that does not require a surface to attach to. Instead, cells self-
108 aggregate to form free-floating suspended biofilms. In another study, the free-floating cellular

aggregates formed by *P. aeruginosa* PAO1 were analyzed by microscopy, with data showing that they comprise up to 90% of the total planktonic biomass, ranging from 10 to 400 μm in diameter, and dispersing into single cells upon carbon, nitrogen, or oxygen limitation (20). During growth, these cellular aggregates contain densely packed viable cells, but upon starvation cell death increases, and metabolites and bacteriophages are released to the supernatant.

In this work, we asked whether the *B. multivorans* ATCC 17616 LTTR (Bmul_2557) identified plays a role at the interface between metabolism and pathogenesis, namely by governing carbon overflow, EPS production, and cellular aggregates/biofilm formation. To address these questions, we made use of a *Bmul_2557* mutant and evaluated EPS production with different carbon sources, measured carbon consumption and metabolic end-products, as well as cellular aggregates and biofilm formation. This LTTR, through direct or indirect regulation of the expression of a D-lactate dehydrogenase encoding gene and possibly other genes, was found to have a significant influence on cellular aggregates and attached biofilm formation, but a negative effect on polysaccharide biosynthesis. Furthermore, it regulated the overflow products generated in excess of glucose and similar sugars. Our data support a role for Bmul_2557 LTTR as a key regulator at the boundary between metabolic performance and virulence of *B. multivorans*.

RESULTS

Expression of *Bmul_2557* gene is decreased in nonmucoid variants. Previous work on the nonmucoid *B. multivorans* D2214 and the clonal mucoid D2095 CF isolates revealed that the gene homolog of *Bmul_2557* from *B. multivorans* ATCC 17676 encoding a putative LTTR had decreased expression in the nonmucoid isolate (16). To assess whether this gene could have a role in the expression of the mucoid phenotype due to cepacian production, its expression level was measured in several stress-induced nonmucoid variants derived from mucoid strains of different *Burkholderia cepacia* complex species (11) grown in S medium with 2% D-mannitol. In agreement with the previous finding in *B. multivorans* D2214/D2095 isolates, the transcription of *Bmul_2557* gene homologue was decreased in all tested nonmucoid variants relative to the respective mucoid parental strain *B. multivorans* D2095, *B. contaminans* IST408, *B. anthina* FC0967, *B. vietnamiensis* PC259, and *B. dolosa* CEP0743 (Fig. 2A).

Bmul_2557 gene, tentatively named *ldhR* (*l*actate *d*e*h*ydrogenase *r*egulator), is located on chromosome 1 of the soil isolate *B. multivorans* ATCC 17616. Downstream and in the same orientation is located gene *Bmul_2558* encoding a putative D-lactate dehydrogenase (LdhA) (Fig. 2B). Comparison of *ldhR* gene upstream region with the one of the characterized homolog *scmR* from *Burkholderia thailandensis* E264, whose expression is known to be induced by quorum sensing and having a *lux*-box (21), shows absence of such conserved region in *B. multivorans* (Fig. 2B). *In silico* analysis predicts an operonic structure for *ldhR* and *ldhA* genes. Reverse transcription PCR experiments on wild-type (WT) cells grown for 18 hours in S medium with D-mannitol confirmed their co-transcription and that *Bmul_2559* belongs to another transcriptional unit (Fig. 2C).

LdhR and LdhA display conserved domains of LTTR regulators and D-lactate dehydrogenases, respectively. *In silico* analysis indicated high conservation of the genomic location of genes *ldhR* and *ldhA* within the *Burkholderia* genus. From the 673 strains whose genome sequence is available at the Burkholderia Genome Database (Mai, 2017), only 9 lack the *ldhR* gene homolog while 18 do not have the *ldhA* gene homolog. None of these 27 strains is from the *Burkholderia cepacia* complex. Homology search at the amino acid level between LdhR and other characterized LTTRs indicated that the highest degree of similarity is within the N-terminal helix-turn-helix domain responsible for binding DNA (Fig. S1A). The best characterized homolog is ScmR of *B. thailandensis* E264, showing 65% identity (77% similarity). Some amino acid residues important for DNA binding identified by mutagenesis in proteins CrgA, CysB and OxyR (22) are also conserved in LdhR from *B. multivorans*. The less conserved C-terminal region, where the co-inducer domain is located, has some homology to sugar-binding domains present in ABC transporters and other sugar-binding proteins, suggesting that a sugar-derived metabolite might be involved in LdhR activation.

Protein LdhA is homologous to members of the superfamily of NAD-dependent D-isomer specific 2-hydroxyacid dehydrogenases. Alignment of the amino acid sequence of LdhA with the one of *B. thailandensis* E264 and other D-lactate dehydrogenases, which had their tridimensional structure determined, showed conservation of important residues in both the nucleotide binding domain and the catalytic domain, as exemplified by the conservation of R^{235} and E^{264} involved in substrate binding, and D^{259} and H^{296} involved in catalysis (Fig. S1B).

To substantiate the putative function of LdhA as a D-lactate dehydrogenase, a phylogenetic analysis of the family of D-isomer specific 2-hydroxyacid dehydrogenases was performed.

173 Based on PROSITE pattern_1 we aligned 185 proteins from the families of D-lactate
174 dehydrogenase (D-LDH), D-3-phosphoglycerate dehydrogenase (SERA), erythronate-4-
175 phosphate dehydrogenases (PDXB), formate dehydrogenase (FDH),
176 glyoxylate/hydroxypyruvate reductases (GHPR), and C-terminal binding protein (CTBP).
177 Phylogenetic analysis shows clustering of the proteins according to substrate specificity, with
178 LdhA from *B. multivorans* ATCC 17616 grouping together with D-lactate dehydrogenases
179 from *E. coli*, *Lactobacillus plantarum*, *Streptococcus agalactiae*, *Staphylococcus aureus*, and
180 *Treponema pallidum* (Fig. 3).
181
182 **LdhR regulator has a negative effect in EPS production.** To test the hypothesis of the
183 LdhR regulator being involved in EPS production, *B. multivorans* ATCC 17616 and the Δ*ldhR*
184 deletion mutant were grown in S medium with different carbon sources for 3 days. In the
185 presence of 2% D-galactose, D-fructose, D-mannitol, or D-mannose, the mutant produced
186 approximately 32-45% more EPS than the WT strain (Fig. 4A). In medium supplemented with
187 2% D-glucose, the WT strain was unable to produce EPS while the Δ*ldhR* mutant produced
188 approximately 6 g/l.
189 To test whether introducing the *ldhR* gene in the mutant would decrease EPS production, a
190 complementation experiment by expressing *ldhR* gene from pMM137-2 was performed. EPS
191 quantification in medium with the different sugars was not significantly different from the
192 mutant carrying the empty vector (data not shown), suggesting a possible polar effect of the
193 trimethoprim resistance cassette replacing *ldhR* gene on the *ldhA* gene expression, as will be
194 demonstrated in the next section. Due to this observation, genes *ldhR* and *ldhA* were expressed
195 simultaneously from their own promoter region cloned into plasmid pARG015-1. When grown

196 in the presence of D-mannose or D-mannitol, there was indeed reduction in the amount of EPS
197 produced either by overexpression of *ldhRA* in the mutant or in the WT (Fig. 4B). In the
198 presence of D-glucose, the Δ*ldhR* mutant expressing *ldhRA* genes produced no EPS, restoring
199 the phenotype of the WT strain. Similarly, overexpression of both genes in the WT strain
200 confirmed the loss of EPS production (Fig. 4B). Expression of *ldhA* gene in the Δ*ldhR* mutant
201 had a similar effect as expressing both *ldhRA* (data not shown). Together, these results suggest
202 a negative effect of *ldhR* and *ldhA* gene products on the biosynthesis of EPS.
203
204 **Deletion of *ldhR* gene has a positive effect on cell viability in glucose-rich medium.** Due
205 to impairment of EPS production by *B. multivorans* ATCC 17616 in medium containing 2% of
206 D-glucose, but not by the Δ*ldhR* mutant, we compared their growth and culture medium pH in
207 the presence of 2% D-mannitol or of 2% D-glucose as carbon sources. No significant difference
208 was observed in the exponential growth phase of both strains in mannitol-rich medium,
209 although the final biomass of the Δ*ldhR* deletion mutant was consistently higher (Fig. 5A). The
210 pH of the culture medium of both strains remained constant for the time of the experiment. In
211 medium with 2% D-glucose, both strains displayed similar growth rates, but when entering
212 stationary phase, the WT culture showed a decrease in optical density (Fig. 5B) as well as cell
213 viability as determined by CFUs count (Fig. 5C). Since it is known that glucose metabolism
214 can lead to medium acidification, we measured the growth medium pH during the course of the
215 experiment. Up to 48 hours, both the WT and the Δ*ldhR* mutant caused a drop in pH, reaching
216 pH 3.5 and pH 4.4, respectively. After that time, the medium pH of the WT culture remained at
217 3.5, whereas the Δ*ldhR* mutant reproducibly increased the culture medium pH to 6.0 by day 3
218 (Fig. 5D). When 0.5% D-glucose was used, no significant differences in growth and viability

were observed, despite the higher biomass of the Δ*ldhR* mutant (Fig. 5B and C). The culture medium pH also remained constant and at a neutral value (Fig. 5D).

Genetic complementation of the Δ*ldhR* mutant by expressing gene *ldhR* under the control of the bce promoter did not restore either the WT impaired cell viability in the presence of 2% D-glucose or the culture medium acidification to around pH 3.5 (Fig. 6A-C). This suggests lack of *ldhR* expression from the plasmid or a polarity effect of the trimethoprim resistance cassette on *ldhA* gene expression. To test these hypotheses we performed quantitative RT-PCR. Data confirmed the expression of *ldhR* gene in the complemented mutant, although the level was lower than the one of the WT strain (Fig. 6D). Overexpression of *ldhR* gene in the WT strain also resulted in increased levels of *ldhR* gene expression, discarding the hypothesis of deficient expression from the bce promoter. Additionally, the expression of *ldhA* gene was decreased both in the Δ*ldhR* mutant and the complemented mutant (Fig. 6D), confirming not only the polarity of the trimethoprim resistance cassette on *ldhA* expression, but also that Δ*ldhR* mutant acts effectively as double *ldhRA* mutant. Nevertheless, *ldhA* gene expression was increased when *ldhR* gene was overexpressed in the WT strain, giving additional support of *ldhR* and *ldhA* genes being in a polycistronic operon and confirming the direct or indirect involvement of LdhR regulator in *ldhA* gene expression. Transcription data of *B. thailandensis* E264 shows 4.8-fold decreased expression of the *ldhA* gene when the upstream gene *scmR* was deleted (21), also supporting our observations in *B. multivorans* ATCC 17616.

Overexpression in the Δ*ldhR* mutant of *ldhA* gene alone (pLM016-2) or together with the *ldhR* gene restored the WT phenotype with a decrease in optical density and cell viability and no recovery of the culture medium pH from 3.5 to 6 (Fig. 6A-C), confirming protein LdhA involvement in these phenotypes. Introduction of each of the three plasmids into the WT strain

242 slightly enhanced the growth negative effects in the presence of 2% D-glucose, being more
243 visible for the strain expressing *ldhRA* genes simultaneously (Fig. S2A-C).

244 Taken together, our data shows that the extreme acidification of the growth medium is
245 possibly the cause of decreased cell viability of WT cells in the presence of 2% D-glucose. This
246 acidification is most likely due to organic acids secretion and in particular to the activity of the
247 D-lactate dehydrogenase LdhA involved in the production of D-lactic acid from pyruvate.

248

249 **The negative effect on cell viability and EPS production in glucose-rich medium is**
250 **prevented by buffering the growth medium.** To confirm that loss of cell viability is
251 dependent on the acidic pH observed, we grew the WT and Δ*ldhR* mutant cells in medium
252 supplemented with 2% of D-glucose buffered with 0.2 M Tris.Cl with an initial pH of 7.2.
253 Under these conditions, the WT and Δ*ldhR* mutant showed similar growth trends and viability,
254 although the Δ*ldhR* mutant exhibited higher final biomass (Fig. S3A-B). The acidification of
255 the growth medium was also observed for both strains, but the lowest pH values obtained were
256 4.8 for the WT strain and 5.3 for the Δ*ldhR* mutant (Fig. S3C). After reaching this minimum,
257 both strains recovered the culture medium pH towards neutrality. EPS production was also
258 quantified after 96 hours of growth in buffered 2% D-glucose containing medium, with the WT
259 strain recovering its ability to produce EPS, despite a reduction of 25% when compared to the
260 Δ*ldhR* mutant **(**Fig. S3D**)**.

261

262 **Cell survival threshold is surpassed by secretion of D-lactate.** To examine whether the
263 pH drop in glucose-rich medium was due to organic acid production, we employed reverse-
264 phase HPLC. By comparing peak retention times with standards, we identified the peaks

265 corresponding to gluconate (GN), 2-ketogluconate (2KG), and D-lactate. In accordance to the
266 pH drop by 48 hours of growth in the presence of 2% D-glucose, both the WT and Δ*ldhR*
267 mutant strains converted GN to 2KG although the concentration was higher for the WT strain
268 (Fig. 7A). In the following hours, 2KG concentration decreases in the Δ*ldhR* mutant, most
269 likely due to its consumption while in the WT strain the levels remained high and constant due
270 to loss of cell viability (Fig. 7A). An inspection of D-glucose consumption shows the same
271 trend for both strains, with no detectable quantity by 48 hours (Fig. 7B). D-lactate increased in
272 the growth medium of the WT strain up to 7 mM at 32 hours, decreased to 5 mM until 48
273 hours and remained the same until the end of the experiment (Fig. 7B). From the Δ*ldhR* mutant
274 supernatant, no D-lactate was detected.

275 Growth of WT and Δ*ldhR* mutant in 0.2 M Tris-buffered medium leads to similar
276 consumption of D-glucose and conversion into 2KG until 48 hours, but then both strains are
277 able to consume this metabolite at similar rate (data not shown). D-lactate concentration
278 increased in the growth medium of the WT strain up to 48 hours, but then it was reduced by
279 consumption and at 72 hours, no D-lactate was detected. From the Δ*ldhR* mutant supernatant,
280 no D-lactate was detected. Overexpression of *ldhR* gene in the WT strain increases the
281 concentration D-lactate in the supernatant, possibly due to a positive effect on the expression of
282 *ldhA* gene (Fig. S2D). When *ldhA* gene is expressed in the WT strain, D-lactate concentration
283 was even higher.

284 Overall, D-glucose metabolism in the WT strain leads to organic acids secretion with a
285 concomitant pH decrease, and if that value reaches a critical level, cells loose viability.
286 Contrastingly, the absence of D-lactate accumulation by the Δ*ldhR* mutant prevents such
287 stronger acidification with cells remaining viable.

288

289 **Enzymatic activities confirm organic acids secretion with Δ*ldhR* mutant displaying**
290 **lower lactate dehydrogenase activity than the WT strain.** Data obtained for organic acids
291 secretion by the WT strain and the Δ*ldhR* mutant was confirmed by measuring key enzymes
292 from the direct oxidative and phosphorylative pathways of D-glucose dissimilation, as well as
293 conversion of pyruvate into lactate. Cells were grown in the presence of 2% D-glucose or D-
294 mannitol to measure activation of one or the other pathway. In general, in the presence of D-
295 glucose the enzymes of the oxidative pathway (GDH and GNDH) have higher specific
296 activities than in D-mannitol-rich medium (Fig. 7C). Conversely, G6PDH activity is higher in
297 D-mannitol rich medium. Comparison of WT and Δ*ldhR* mutant showed no difference in the
298 enzymatic activity of the tested enzymes, except lower decreased activity in the mutant of GDH
299 and G6PDH in medium supplemented with D-glucose and D-mannitol, respectively (Fig. 7C).
300 Total lactate dehydrogenase activity (LDH) in crude extracts revealed lower specific activity in
301 the Δ*ldhR* mutant when compared with the WT, in both D-glucose and D-mannitol-rich medium
302 (Fig. 7C). This result confirms the involvement of D-lactate dehydrogenase LdhA in the WT
303 cells ability to convert pyruvate into D-lactate.

304

305 **Growth medium acidification depends on the metabolized sugar and is strain**
306 **dependent.** To test whether the involvement of LdhR in relieving carbon overflow was
307 specific for D-glucose or also involved other sugars, we grew the WT and Δ*ldhR* mutant in
308 medium supplemented with other carbon sources. Growth in the presence of sugars
309 metabolized by the phosphorylative pathway (Fig. 1) such as D-fructose and D-mannitol,
310 resulted in no medium acidification for both tested strains while D-mannose led to a slight pH

311 decrease of the culture medium. No D-lactate, 2KG, and GN were detected either in the WT or
312 the Δ*ldhR* mutant (data not shown). Growth of the two strains in the presence of another sugar
313 metabolized by the direct oxidative pathway (Fig. 1) such as D-galactose led to culture medium
314 pH acidification to a minimum of 5.2 in the WT strain and 5.5 in the Δ*ldhR* mutant at 48 hours,
315 with both strains recovering to neutrality by 72 hours. D-lactate was identified in the
316 supernatant of the WT, but not of the Δ*ldhR* mutant (data not shown). The consumption rate of
317 the several sugars measured at 48 hours of growth shows that while D-glucose is depleted, for
318 the other sugars there is still considerable amount of the initial concentration and no significant
319 differences were observed between WT and Δ*ldhR* mutant (Fig. 7D). This data shows that
320 metabolic overflow is only caused by the high D-glucose dissimilation rate.
321 Next, we tested whether the negative effect on cell survival registered in the presence of 2%
322 D-glucose was unique for *B. multivorans* ATCC 17616 or it was a more common phenomenon
323 in the *B. cepacia* complex. Eighteen additional strains were tested regarding the minimum pH
324 value reached in the culture medium and whether they recovered to higher pH values, and if D-
325 lactate was produced and consumed. Data shown in Table 1 indicates that only three strains (*B.*
326 *multivorans* VC3161, D2095, and *B. dolosa* CEP1010) had the same behavior as *B.*
327 *multivorans* ATCC 17616, namely culture medium pH decrease to 3.5-3.7 and no recovery,
328 and D-lactate secretion but no consumption. A second group of ten strains (*B. multivorans* JTC,
329 VC7495, VC6882, VC12539, VC8086, VC9159, VC12675, *B. ambifaria* CEP0996, *B. stabilis*
330 LMG 14294, and *B. cenocepacia* ATCC 17765) showed minimum culture medium pH values
331 ranging from 4.0-6.3, but this value increased towards neutrality. All these strains secreted D-
332 lactate into the growth medium during the first 48 hours, but it was consumed in the following
333 hours. From the last group of five strains (*B. anthina* J2552, *B. cenocepacia* J2315, *B. cepacia*

334 ATCC 25416, *B. contaminans* IST408, and *B. vietnamiensis* G4) we were unable to detect D-
335 lactate, but the culture medium pH decreased to values ranging 4.5-6.5 and then increased to
336 neutrality (Table 1). Enzymatic activities of GDH, GNDH, G6PDH, and LDH in *B. dolosa*
337 CEP1010 (51.7 (± 9.8), 16.0 (± 1.3), 11.2 (± 2.9), and 119.2 (± 12.5) nmoles min^{-1} mg^{-1},
338 respectively) and *B. cenocepacia* ATCC 17765 (15.5 (± 0.8), 5.0 (± 0.4), 52.6 (± 3.7), and 97.4
339 (± 8.8) nmoles min^{-1} mg^{-1}, respectively) grown in medium with 2% D-glucose confirmed
340 differential use of both D-glucose dissimilation pathways. Together, this data suggests that
341 most of the tested strains use the direct oxidative pathway for D-glucose utilization, but some
342 might use the phosphorylative pathway only or a combination of both.
343

344 **Growth in glucose-rich medium induces higher stress to WT than to Δ*ldhR* mutant**
345 **cells.** During the first 24 hours of growth in medium containing 2% D-glucose, organic acids
346 secretion by *B. multivorans* ATCC 17616 and the Δ*ldhR* mutant differed mainly by the
347 presence of D-lactate in the WT culture medium and absence in the mutant and consequently a
348 lower medium pH in the former. To understand the physiological adaptations under these
349 acidic conditions and identify genes being possibly under control of the LdhR regulator,
350 expression profiling studies were performed. The transcriptomes of the Δ*ldhR* mutant and WT
351 strain grown in medium with 2% D-glucose were determined at 22 hours of growth with the pH
352 of the culture medium being of 5.2 for the WT and 6.0 for the Δ*ldhR* mutant. A total of 132
353 genes were differentially expressed, 15 with increased expression and 117 genes with
354 decreased expression (≥1.2-fold lower confidence bound change with a false discovery rate of
355 ≤4.6 %) (Table S1).

356 Among the genes with increased expression in the mutant we found genes *glnL* and *glnB-1*,
357 encoding a signal transduction histidine kinase and the nitrogen regulatory protein P-II,
358 respectively, as well as genes for the acquisition of inorganic (*amt*, *narK*) and organic nitrogen
359 (*urtA*) (Table 2). Genes encoding nitrogen assimilating enzymes such as *nirB*, *nirD* and *glnA*
360 were also upregulated in the mutant strain, suggesting higher needs of nitrogen for anabolic
361 reactions. When compared to the WT growth, the mutant strain is in a more favorable
362 environment since the culture medium is at higher pH. That is reflected in the downregulation
363 of many genes related to stress response, RNA metabolism and protein synthesis (Table 2).
364 Regarding stress response we observed the downregulation of *rpoH* gene encoding RNA
365 polymerase factor sigma-32, as well as several genes encoding peptidases/proteases
366 (Bmul_0546, *lon*, *clpB*), heat-shock proteins (Bmul_2055, Bmul_2056, Bmul_2384, *hslU*,
367 *grpE*) and chaperones (*groEL*, *groES*, *dnaK*), and *katE* gene encoding catalase. Genes whose
368 products are involved in synthesis (*rpoZ* gene encoding the omega subunit of DNA-directed
369 RNA polymerase) or degradation (*dnaK*, *groEL* and *hfq2*) of RNA showed decreased
370 expression in the Δ*ldhR* mutant. In the same line of evidence, 31 genes of ribosomal proteins,
371 the *infC* gene encoding a translation initiation factor IF-3, *thrS* encoding threonyl-tRNA
372 synthetase and *map* gene encoding a methionine aminopeptidase were downregulated in the
373 mutant (Table S1). In terms of central metabolic pathways few differentially expressed genes
374 were found. Of relevance is the increased expression of *cydA* in the WT. This gene encodes the
375 cytochrome bd ubiquinol oxidase subunit I, an enzyme less prone to inhibition by oxidative
376 stress, enabling aerobic metabolism to continue under adverse conditions. Regarding secondary
377 metabolism, there is a cluster of genes (*Bmul_5943* to *Bmul_5949*) whose expression is
378 downregulated in the Δ*ldhR* mutant (Table 2). The products of these genes are homologous to

379 methyltransferases, cytochrome P450, and Rieske (2Fe-2S) domain-containing proteins and
380 might be required for the production of an unknown metabolite. It is also of notice the
381 decreased expression in the Δ*ldhR* mutant of adhesin BapA which has been implicated in
382 biofilm formation.
383

384 **LdhR is required for planktonic cellular aggregates formation and adhesion to**
385 **surfaces.** During aerobic batch growth we observed striking differences between the WT and
386 the Δ*ldhR* mutant. After 72 hours of growth in the presence of 0.5% or 2% of sugars like D-
387 glucose, D-galactose, D-fructose, D-mannitol, and D-mannose, we notice the formation of
388 macroscopic cellular aggregates by the WT strain *B. multivorans* ATCC 17616. These cellular
389 aggregates could reach up to 2-3 mm diameter after 3 days of growth. In contrast, the Δ*ldhR*
390 mutant generated a more homogeneous cell suspension with occasional small aggregates (Fig.
391 S4A).
392 To determine when these planktonic cellular aggregates started to form, WT and Δ*ldhR*
393 mutant strains were incubated in liquid medium containing 2% D-glucose for 24 hours and
394 samples analyzed by microscopy. Wild-type strain planktonic aggregates of different sizes
395 were visible at 4 hours incubation (size range of 3-30 μm) and its number and size increased
396 until the end of the experiment (size range 50-1000 μm) (Fig. 8A). Contrastingly, the Δ*ldhR*
397 mutant was able to form aggregates by 24 hours, but their size range was within 10-60 μm.
398 Similar results were obtained for both strains when D-mannitol (not shown) or D-fructose were
399 used in the growth medium (Fig. S4B).
400 To understand whether cellular aggregates formation is also dependent on the expression of
401 *ldhA* gene encoding a D-lactate dehydrogenase, the WT and Δ*ldhR* mutant were complemented

with genes *ldhR* or *ldhA* alone or simultaneously and grown in liquid medium containing D-mannitol. Microscopy analysis of the aggregates formed by the WT overexpressing the different genes showed dense aggregates with irregular surfaces with numerous ramifications for all of them (Fig. 8B). Planktonic aggregates formed by the Δ*ldhR* mutant with the empty vector or expressing *ldhR* gene alone are of a small size, but when *ldhA* is co-expressed with *ldhR*, aggregates of higher dimension and ramification are evident (Fig. 8B). Expression of *ldhA* gene alone in Δ*ldhR* mutant restored the formation of macroscopic cellular aggregates, but in lower number than complementation with *ldhRA*. This result suggests that planktonic cell aggregation also depends on *ldhA* gene product activity, but it is not the only determinant.

To evaluate whether adhesion to surfaces in the form of biofilms was also altered, the WT and Δ*ldhR* mutant complemented with the several genes were grown in 24-well plates with agitation for 24 hours in medium supplemented with D-mannitol. Results shown in Figure 8C indicate that biofilm formation is approximately 40% lower in the Δ*ldhR* mutant when compared to the WT strain (P <0.001). An image of the plastic surface before crystal violet staining shows macroscopic WT aggregates attached to surface while the Δ*ldhR* mutant formed a smooth surface (Fig. 8C). Complementation of the Δ*ldhR* mutant with *ldhA* gene had slight, but statistically significant (P <0.05), increase in biofilm formation while complementation with both *ldhRA* genes fully recovered biofilm formation to levels even higher than the WT strain. Overexpression of *ldhR* or *ldhA* alone in the WT strain had a small increase in biofilm formation, but when both genes were expressed this increase was of 45% (Fig. 8C). Together, these results suggest that LdhR is relevant for surface attached biofilm formation, and although the D-lactate dehydrogenase activity of LdhA protein contributes to it, is not the only factor affecting biofilm formation.

425

426 **Planktonic aggregates formation is a trait shared by several *B. cepacia* complex**
427 **strains.** To evaluate whether planktonic aggregates are common across the *B. cepacia*
428 complex, we tested 74 additional strains from 9 different species, most of them isolated from
429 CF patients´ lung infections, and we included also 4 different *P. aeruginosa* strains.
430 Microscopy analysis revealed that 40 out of 74 *Burkholderia* strains showed cellular
431 aggregates larger than 10 μm when grown in medium containing 2% D-mannitol for 48 hours
432 with agitation (Fig. 9). The size and structure of the aggregates was variable and strain specific.
433 *B. multivorans*, *B. ambifaria* and *B. contaminans* were the species with more strains being able
434 to form planktonic cellular aggregates. The four *P. aeruginosa* strains tested, all isolated from
435 CF patients´ infections, were also able to form cellular aggregates of different sizes (Fig. 9,
436 panel Q and R). This analysis shows that a considerable number of CF pathogens can grow as
437 planktonic cellular aggregates in addition to single cells.

438 Finally, to evaluate whether EPS plays a role in cellular aggregate formation, the mucoid *B.*
439 *multivorans* VC5602 and a nonmucoid mutant derivative with a frameshift mutation in the
440 *bceF* gene required for EPS biosynthesis were grown for 3 days in D-mannitol rich-medium.
441 After inspection of the cultures, we found planktonic cellular aggregates in both strains,
442 indicating that EPS was not relevant for cellular aggregate formation under the conditions
443 tested.

444

445

446 **DISCUSSION**

447 This work presents the functional analysis of *B. multivorans* ATCC 17616 LdhR regulator
448 and the D-lactate dehydrogenase LdhA. Despite the same genetic organization and high
449 homology levels with ScmR and LdhA from *B. thailandensis* E264, there are striking
450 differences between them. One important difference might be the dependence of quorum
451 sensing (QS) to induce *scmR* (21), but not *ldhR* gene expression. Although we cannot exclude
452 the possibility of *ldhR* expression being QS-dependent, the lack of a *lux*-box sequence in the
453 *ldhR* upstream region and the detection of D-lactate during exponential growth phase give
454 support to the non QS-dependency of *ldhR* gene expression. Other striking differences are in
455 virulence and biofilm formation. While ScmR represses virulence in *Caenorhabditis elegans*
456 and biofilm formation (21), we found no differences between WT and Δ*ldhR* mutant when
457 infecting *Galleria mellonella* larvae (data not shown) and our observations implicate LdhR as
458 an activator of biofilm formation. Furthermore, ScmR is both a repressor and activator of
459 secondary metabolism (regulate the synthesis of peptides, bacteriocins, acids) while our
460 transcriptomic data suggests LdhR as being required for the expression of perhaps only one
461 cluster of genes possibly involved in some unknown secondary metabolite production. Despite
462 these differences between the regulatory networks controlled by the two regulators, both
463 studies showed the upregulation of several genes involved in stress response in the WT cells.
464 Altogether, our work and the one of Mao and coworkers shows an interesting example on how
465 subtle changes in regulatory and/or coding sequences of otherwise similar regulatory proteins,
466 can affect differently the same phenotypes, preventing general conclusions on their role among
467 different (but related) species.

468 Although *B. multivorans* LdhR does not seem to have such strong involvement in secondary
469 metabolism as ScmR, it still has an important role in regulating carbon overflow, especially
470 when D-glucose is used as carbon source. The metabolism of D-glucose by *B. multivorans*
471 ATCC 17616 (formerly *Pseudomonas cepacia* 249) was investigated previously (14). These
472 authors estimated that the rate of dissimilation of glucose to gluconate and 2-ketogluconate via
473 the direct oxidative pathway exceeds the rate of conversion of glucose to glucose-6P via the
474 phosphorylative pathway by a factor of at least 12, concluding that the predominant route of
475 glucose utilization in this strain is the direct oxidative pathway. Furthermore, they also reported
476 the culture medium acidification in the presence of D-glucose. Our data fully confirm these
477 observations, but we further demonstrated that medium acidification is caused by accumulation
478 of gluconate, 2-ketogluconate, and D-lactate, and this strong pH decrease leads to loss of cell
479 survival. Similarly to D-glucose, D-galactose utilization in *B. multivorans* ATCC 17616 also
480 resulted in D-lactate secretion, but the culture medium pH never decreased below a critical level
481 and cells were able to adapt and resume growth. The most likely explanation is the lower rate
482 of D-galactose consumption when compared to D-glucose as shown in Figure 7D.
483 Our data on the consumption of sugars such as D-fructose and D-mannose, and the sugar-
484 alcohol D-mannitol by *B. multivorans* ATCC 17616 showed their dissimilation through the
485 phosphorylative pathway. These compounds are transported across the plasma membrane,
486 converted into fructose-6P prior to gluconate-6P formation and entering the Entner-Doudoroff
487 pathway (Fig. 1). Possibly due to transport limitations and/or enzymatic activity of the
488 phosphorylative pathway enzymes, the consumption rate of these sugars is considerably lower
489 when compared to D-glucose. As a consequence, no accumulation of organic acids was
490 detected and the culture medium pH remained close to neutrality.

491 The role of LdhR, and especially LdhA, in carbon overflow seems to be dependent on the
492 sugar being consumed and on the dissimilation rate. The faster catabolism of D-glucose and D-
493 galactose (to a lesser extent) by the Entner-Doudoroff pathway leads to increased formation of
494 glyceraldehyde-3P and pyruvate. To regenerate the NADH used in the previous reactions,
495 pyruvate is converted into lactate (and possibly other acids) which is also secreted to the culture
496 medium, further contributing to the extracellular acidification observed in the WT strain. In the
497 absence of LdhR and consequently also the absence of D-lactate dehydrogenase LdhA activity
498 (although there was still lactate dehydrogenase activity in the crude extracts), no secretion of D-
499 lactate was observed and the drop in pH was attenuated. The absence of carbon overflow
500 caused by the slower catabolism of sugars that use the phosphorylative pathway puts lower
501 pressure into NADH regeneration, and LdhA might have a more limited role in regulating
502 metabolic fluxes.

503 We have shown that growth of several strains from different species of the *B. cepacia*
504 complex reveals a strain-dependent utilization of a pathway for D-glucose dissimilation. These
505 differences might be caused mainly by the enzymatic activity of glucose dehydrogenase. Lessie
506 and coworkers have shown that *B. multivorans* ATCC 17616 expressed the enzyme glucose
507 dehydrogenase constitutively (23). Our enzymatic activity on the same strain and in *B. dolosa*
508 CEP1010 confirmed this result. In addition, we observed that *B. cenocepacia* ATCC 17765
509 which has a much lower level of glucose dehydrogenase activity, has an increase of glucose-6P
510 dehydrogenase activity and is most likely using the phosphorylative pathway for D-glucose
511 dissimilation. These differences in D-glucose consumption might be relevant in an environment
512 where several organisms compete for the same carbon sources. The fast conversion of glucose
513 into less accessible compounds such as gluconate and 2-ketogluconate, together with the

514 lowering of the surrounding pH will certainly exclude some competitors. Another advantage is
515 that protons generated from these oxidation steps contribute directly to transmembrane proton
516 motive force and therefore to ATP synthesis (24).

517 Expression data showed that another side effect of organic acids secretion when cells are
518 grown in excess of D-glucose is the induction of a stress response possibly against intracellular
519 acidification. Since the pK_a for D-lactate, gluconate and 2-ketogluconate is 3.86, 3.39 and 2.67,
520 respectively, a major cause of intracellular acidification might be the entrance of D-lactic acid.
521 Our data shows that cultures where the pH stayed above 4 (Table 1) were still able to survive
522 and resume growth, but once the pH was below this value, cells lost viability rapidly. D-lactate
523 is a weak acid which means that an increase of the undissociated form occurs with lowering of
524 the pH. This undissociated form is capable of diffusing through the cell membrane, affecting its
525 structure and causing intracellular acidification as the acid dissociates in the cytosol and
526 releases protons. The Δ*ldhR* mutant grown in excess of D-glucose lowers the culture medium
527 pH to 4.4, but this value seems to be harmless because cells continue growth and eventually
528 consume the organic acids. This different behavior is reflected in the transcriptomic data which
529 confirms the stronger (although inefficient under our *in vitro* conditions) induction of stress
530 response mechanisms, including increased expression in the WT of the gene encoding the heat
531 shock response transcriptional regulator RpoH, as well as several genes encoding heat shock
532 proteins, chaperones and the proteases ClpB, ClpS, Lon and HslU. An increase of these
533 proteins in the cell would help to fold proteins and degrade the denatured ones. A study of the
534 sigma factor RpoH1 in the regulation of *Sinorhizobium meliloti* genes upon pH stress also
535 identified several RpoH1-dependent genes as differentially expressed, including the
536 upregulation of genes encoding heat shock proteins like IbpA, GrpE, GroEL5, Hsp20, proteases

such as ClpA, ClpB, ClpS1, ClpP2, ClpX, DegP1, Lon, and HslV, as well as the downregulation of genes involved in translation and nitrogen metabolism like NarB, NirB, NirD, GlnK (25). The upregulation of stress response genes in the WT *B. thailandensis* E264 is attributed as an adaptation to stationary phase (21). Yet, it cannot be excluded that this induction of stress response gene expression might result from the presence of high concentration of toxic secondary metabolites in the culture medium.

One of the main findings implicates LdhR and, to a certain extent, also LdhA in planktonic cellular aggregates formation. These aggregates are free-floating biofilm-like structures not requiring a surface to attach to. Growth of *P. aeruginosa* PAO1 in liquid batch cultures confirmed the preferential formation of planktonic cellular aggregates during the growth phase as opposed to free cells, but under stress conditions, such as the ones imposed by nutrient limitation these aggregates disperse into single cells as reflected by an increase in optical density (20). Contrastingly to *P. aeruginosa*, we did not observe the sudden increase of optical density at the beginning of the stationary phase and the number/size of the *Burkholderia* aggregates continued to increase with time. Planktonic cellular aggregates are particularly relevant for bacteria infecting the CF lungs as it has been shown that *P. aeruginosa* is found in lung tissues near the epithelial cell surface as non-surface attached microcolonies (18). In another study that examined *P. aeruginosa* and *B. cepacia* complex infected CF lung tissues by immunostaining, *P. aeruginosa* was found in the form of microcolonies while *B. cepacia* complex bacteria were found both as single cells and as cellular aggregates (2). At least two regulators have been shown to influence microcolony formation by *P. aeruginosa*. One of them is the LTTR BvlR whose inactivation prevented microcolony formation, but the mechanism is unknown (19). The other identified regulator is the two-component regulator MifR, with the

560 *mifR* mutant biofilms exhibiting thin, structure lacking microcolonies (17). This phenotype was
561 dependent on pyruvate utilization since inactivation of genes encoding lactate dehydrogenase
562 and aconitate hydratase abrogated microcolony formation in a manner similar to *mifR*
563 inactivation, suggesting that fermentation of pyruvate is required for microcolony formation.
564 An explanation is that within microcolonies *P. aeruginosa* cells experience oxygen limiting but
565 energy rich conditions and use pyruvate fermentation as a means of redox balancing allowing
566 microcolony formation and biofilm development (17). The contribution of D-lactate
567 dehydrogenase for *B. multivorans* ATCC 17616 planktonic aggregates and biofilm formation
568 might also be due to the anoxic environment in the interior of the aggregate, inducing cells to
569 ferment pyruvate as a means of redox balancing. Nevertheless, LdhA activity is not the only
570 factor involved in cellular aggregates and biofilm formation, as shown by the partial
571 complementation of these phenotypes by the mutant strain. Adhesin BapA might also
572 contribute to the formation of these planktonic cell aggregates and biofilms, since its expression
573 was upregulated in the WT strain. This adhesin has been implicated in *B. cenocepacia*
574 microcolony formation and its inactivation gave rise to a porous and disconnected biofilm (26).
575 A study carried out in *B. thailandensis* showed the role of C8-homoserine lactone in cell
576 aggregation once a sufficient population number was reached, implicating quorum-sensing in
577 the self-aggregation phenotype (27). Further studies need to be done in *B. multivorans* to assess
578 these possibilities.

579 Our data showing higher biofilm formation ability of the WT strain, with visible aggregates
580 attached to the surface, in contrast to the smooth biofilm formed in lower amount by the Δ*ldhR*
581 mutant is in line with a study to determine the relative fitness of single cells and preformed
582 aggregates during early development of *P. aeruginosa* biofilms, which showed a single cells

583 density-dependent fitness of the aggregates (28). These authors showed that when growth
584 resources are abundant, aggregates have a disadvantage because the aggregate´s interior has
585 poor access to resources. However, if competition for resources is high, aggregates have higher
586 fitness because they can protrude above the surface and cells at the top of the aggregate have
587 better contact to growth resources. Another possible link between biofilm formation and the
588 LdhR regulator was observed for an experimentally evolved *B. cenocepacia* HI2424 biofilm
589 during 1050 generations of selection (29). Mutation analysis revealed early beneficial
590 mutations in the gene encoding the LdhR homologue (Bcen2424_0826), generating new
591 haplotypes. Three different mutations were identified in the three ecotypes and consisted of a
592 two-codon deletion and a SNP (Δ38A, Δ39M, L40V) which mapped into the DNA-binding
593 domain (Fig. S1A). The effect of these mutations in the DNA-binding ability of the regulator
594 and its effect on gene expression are unknown. These observed mutations might be beneficial
595 for growth in the D-galactose minimal medium used in that study, but can also reflect selection
596 for biofilm production.

597 The production of EPS, namely cepacian, is a widespread trait in the *B. cepacia* complex
598 bacteria (6, 7). Although the genes encoding the proteins involved in cepacian biosynthesis are
599 well known (5), the regulatory elements controlling the expression of this phenotype remain
600 unknown. The exception is the regulator σ^{54} which has been shown to positively regulate EPS
601 production in *B. cenocepacia* grown under nitrogen starvation (30). Here, we have shown a
602 negative effect in EPS biosynthesis by LdhR and LdhA, but this might be a consequence of
603 planktonic cellular aggregates formation. Cells of the Δ*ldhR* mutant grow as single cells and
604 small aggregates and most of them contribute to EPS production. Contrastingly, WT aggregates
605 are much larger and possibly have smaller contributions to EPS biosynthesis, explaining the

606 lower yield in the presence of carbon sources such as D-mannitol, D-mannose, and D-fructose.
607 Additionally to cell aggregation having an influence in EPS biosynthesis, we observed that EPS
608 production does not seem to influence planktonic aggregate formation. Indeed, the EPS
609 producer *B. multivorans* VC5602 and its isogenic mutant VC5602-nmv1 deficient in EPS due
610 to a mutation in *bceF* gene, both form aggregates, although we did not assess whether they are
611 structurally similar. The downregulation of *ldhR* gene expression in nonmucoid isolates can be
612 explained as a genetic program for adaptation to different oxygen tensions. During growth in
613 liquid medium, nonmucoid cells are not exposed to significant limitation to oxygen diffusion,
614 while the presence of EPS surrounding mucoid cells would create a somewhat less aerated
615 environment. In this last circumstance, cells might sense some degree of oxygen limitation and
616 induce alternative ways, such as pyruvate fermentation, to obtain energy.

617 Although *ldhR* or *ldhA* genes were not found as mutated in serial isolates of *B. multivorans*
618 and *B. dolosa* sampled from long-term CF lung infections (31, 32), a possible role in these
619 persistent infections where oxygen gradients are present and fermentation is an alternative to
620 obtain energy, cannot be excluded. The observation of *B. cepacia* complex bacteria being
621 present in the mucus layer also as cell aggregates (2) is an indication of the relevance of this
622 type of growth, possibly providing additional resistance against antimicrobials and the immune
623 system. Since planktonic cellular aggregates formation was observed in almost all tested *B.*
624 *cepacia* complex species and in more than 50% of the CF isolates analyzed, these are good
625 indications on the possible role of LdhR and LdhA as persistence determinants, and more
626 research into their function is needed.

627 In conclusion, we have shown that the LTTR LdhR and the D-lactate dehydrogenase LdhA
628 are implicated in planktonic cellular aggregates and in biofilm formation, a property possibly

629 relevant in natural environments and within hosts. These cellular aggregates have decreased
630 oxygen gradients towards the center and fermentation of pyruvate would allow these cells to
631 stay viable. We also showed the role of LdhA in the production of D-lactate to decrease the
632 overflow of metabolic intermediates caused by dissimilation of excess of sugars such as D-
633 glucose and D-galactose. The fast catabolism of preferred carbon sources into organic acids is
634 especially advantageous in natural environments. Overall our findings evidence the important
635 role of LdhR regulatory circuits for cell adaptation to diverse environments.
636

637 **MATERIALS AND METHODS**

638 **Bacterial strains and growth conditions.** The bacterial strains and plasmids used in this
639 study are described in Table 3. *E. coli* was grown at 37°C in Lennox Broth (LB) with or
640 without agar, supplemented with kanamycin (50 µg/ml), trimethoprim (50 µg/ml), or
641 chloramphenicol (25 µg/ml) when required to maintain selective pressure. *Burkholderia* strains
642 were grown in LB or in S medium (12.5 g/l $Na_2HPO_4.2H_2O$, 3 g/l KH_2PO_4, 1 g/l K_2SO_4, 1 g/l
643 NaCl, 0.2 g/l $MgSO_4.7H_2O$, 0.01 g/l $CaCl_2.2H_2O$, 0.001 g/l $FeSO_4.7H_2O$, 1 g/l yeast extract, 1
644 g/l casamino acids, pH 7.2) (33) supplemented with 2% (w/v) of one of the following carbon
645 sources: D-glucose, D-mannitol, D-galactose, D-mannose, or D-fructose at 37°C with 200 rpm
646 of orbital agitation. Growth medium for *B. multivorans* was supplemented with the following
647 antibiotics: trimethoprim (100 µg/ml), ampicillin (100 µg/ml), and chloramphenicol (200
648 µg/ml).

649

650 **DNA manipulation and cell transformation techniques.** Genomic DNA from
651 *Burkholderia* was extracted by using the DNeasy blood and tissue kit (Qiagen), following the
652 manufacturers' recommendations. Plasmid DNA isolation and purification, DNA restriction,
653 agarose gel electrophoresis, DNA amplification by PCR, and *E. coli* transformation were
654 performed using standard procedures (34). *Burkholderia* electrocompetent cells were
655 transformed by electroporation using a Bio-Rad Gene Pulser II system (200 Ω, 25 µF, 2.5 kV)
656 and grown overnight before being plated on selective medium. Triparental conjugation to *B.*
657 *multivorans* strains was performed using the helper plasmid pRK2013.

658

659 **Mutant construction**. The 1791-bp HindIII/XbaI upstream region of *ldhR* (*Bmul_2557*)
660 gene was amplified by PCR from *B. multivorans* ATCC 17616 genomic DNA using the
661 primers Bmul2557L (fwd/rev) (Table 4). After digestion with the appropriate restriction
662 endonucleases, the fragment was cloned into pBCKS vector giving rise to pAT312. The 1800-
663 bp XbaI/SacI downstream region of *ldhR* was amplified using the primers Bmul2557R and
664 cloned into the same restriction sites of pAT312 and the resulting plasmid was named pAT812.
665 A fragment containing the trimethoprim resistance cassette from pUC-TP was then cloned into
666 the *Xba*I site of pAT812 originating pAT812-Tp. To delete the gene *ldhR* from *B. multivorans*
667 ATCC 17616, pAT812-Tp was introduced into this strain by electroporation. Recombinant
668 colonies were first selected in the presence of trimethoprim and counter selected in a medium
669 supplemented with chloramphenicol. Gene deletion was confirmed by PCR amplification
670 followed by DNA sequence determination.
671
672 **Complementation assays.** A 1,070-kb NdeI/XbaI fragment containing *ldhR* gene was
673 amplified by PCR from *B. multivorans* ATCC 17616 genomic DNA using primers P1 (fwd/rev)
674 (Table 4). The fragment was cloned into the NdeI/XbaI restriction sites of pLM135-5, a
675 pUK21-derivative plasmid carrying 0.4-kb containing the bce promoter region directing the
676 expression of the *bce* operon required for cepacian biosynthesis. The resulting pMM137-1
677 intermediate plasmid was digested with HindIII and XbaI and the 1.47-kb fragment containing
678 the bce promoter and *ldhR* gene was cloned into vector pBBR1MCS, resulting in plasmid
679 pMM137-2 (Table 3**)**. The same strategy was used to clone *ldhA* gene (amplified with P2
680 (fwd/rev) primers) under the control of the bce promoter, resulting in plasmids pLM016-1 and
681 the final pLM016-2. To clone the *ldhRA* genes under the control of their own promoter, a 2.7-

682 kb fragment of *B. multivorans* ATCC 17616 genome containing the upstream region of *ldhR*
683 and the coding sequence of *ldhR* and *ldhA* genes was amplified by PCR using P3 (fwd/rev)
684 primer sequences. The amplified DNA was restricted with HindIII and ligated to pBBR1MCS
685 originating plasmid pARG015-1 (Table 3). After *E. coli* DH5α transformation and clone
686 selection, the inserted genes were confirmed by DNA sequence determination. Plasmids
687 pMM137-2, pLM016-2 and pARG015-1 were mobilized into *B. multivorans* ATCC 17616 and
688 the Δ*ldhR* mutant by triparental conjugation. Transformants were selected in LB plates
689 supplemented with 100 µg/ml of ampicillin and 200 µg/ml of chloramphenicol.
690
691 **Isolation of RNA samples.** For qRT-PCR and microarray analyses, cells were grown in S
692 medium with 2% D-mannitol or D-glucose for 22 hours at 37ºC. For reverse transcription-PCR
693 cells were grown for 18 hours in S medium supplemented with 2% D-mannitol under the same
694 conditions. Three biological replicates were obtained for each tested strain. For RNA analysis
695 bacterial cells were resuspended in RNAprotect bacteria reagent (Qiagen), and total RNA
696 extraction was carried out using the RNeasy MiniKit (Qiagen) by following manufacturer's
697 recommendation. RNA was treated with DNase (RNAse-free DNAse, Qiagen) for 1 hour at
698 room temperature following manufacturer's protocol and total RNA concentration was
699 assessed using NanoDrop ND-1000 spectrophotometer. RNA integrity for microarray analysis
700 was checked on an Agilent 2100 Bioanalyser using an RNA Nano assay.
701
702 **Quantitative real-time RT-PCR.** Total RNA was used in a reverse transcription reaction
703 with TaqMan Reverse Transcription Reagents (Applied Biosystems). qRT-PCR amplification
704 of genes *ldhR*, *ldhA*, and *trpB* (for primer sequence see Table 4) was performed with a model

705 7500 thermocycler (Applied Biosystems). The expression ratio of the target genes relative to
706 the reference gene *trpB*, which showed no variation in the transcription abundance under the
707 conditions tested, was determined. Relative quantification of gene expression by real-time
708 qRT-PCR was determined using the $\Delta\Delta C_t$ method (35).
709
710 **Reverse transcription-PCR.** To evaluate if *ldhR* and *ldhA* genes are co-transcribed, a
711 semi-quantitative RT-PCR was performed. Total RNA from *B. multivorans* ATCC 17616
712 grown in S medium supplemented with D-mannitol for 18 hours at 37ºC 200 rpm was
713 extracted. A total of 200 ng of total RNA was used for reverse-transcription reaction using
714 Taqman reagent kit (Applied Biosystems, Roche). Synthesized cDNA was used as template for
715 25-µl PCR reactions with 0.2 µM primers 2557/2558_RT or 2558/2559_RT (Table 4), 0.2 mM
716 deoxynucleosides triphosphate, 1.6 mM $MgSO_4$, 1× PCR amplification buffer, and 2.5 U of
717 Taq polymerase (Bioline). Amplification occurred as following: initial denaturation at 95ºC for
718 5 minutes; 30 cycles of 30 seconds at 95ºC, 45 seconds at 52ºC, and 30 seconds at 72ºC; final
719 extension at 72ºC for 10 minutes.
720
721 **Processing of RNA samples for transcriptomic analysis.** Total RNA was processed for
722 use on Affymetrix custom *Burkholderia* arrays, according to the manufacturer's Prokaryotic
723 Target Preparation Assay as described previously (16). Biological triplicates of RNA from
724 each bacterial culture were processed and analyzed.
725
726 **Microarray analysis.** Scanned arrays were analyzed with Affymetrix Expression Console
727 software to guarantee that all quality parameters were in the recommended range. Subsequent

728 analysis was performed with DNA-Chip Analyzer 2008. Since the used custom arrays
729 represents two different *Burkholderia* species (16), a digital mask leaving for analysis only the
730 9610 probe sets representing *B. multivorans* ATCC 17616 transcripts was applied. Then the 6
731 arrays were normalized to a baseline array with median CEL intensity by applying an Invariant
732 Set Normalization Method (36). Normalized CEL intensities of the arrays were used to obtain
733 model-based gene expression indices based on a Perfect Match (PM)-only model (37).
734 Replicate data (triplicates) for each bacterial isolate was weighted gene-wise by using inverse
735 squared standard error as weights. All genes compared were considered to be differentially
736 expressed if the 90% lower confidence bound of the fold change (LCB) between experiment
737 and baseline was above 1.2. The lower confidence bound criterion meant that we could be 90%
738 confident that the fold change was a value between the lower confidence bound and a variable
739 upper confidence bound. Li and Wong have shown that the lower confidence bound is a
740 conservative estimate of the fold change and therefore more reliable as a ranking statistic for
741 changes in gene expression (36).
742
743 **Exopolysaccharide quantification.** The amount of EPS was assessed based on dry weight
744 of the ethanol-precipitated polysaccharide recovered from triplicates of 100 ml culture samples
745 of the different strains grown in liquid S medium supplemented with 2% (w/v) of different
746 sugars over 3 days at 37°C with 200 rpm of orbital agitation as previously described (33).
747
748 **Determination of carbon source and organic acids concentration in the culture**
749 **medium.** The supernatant of each culture (2 ml) was obtained by centrifugation at 14,000 *g* for
750 10 minutes followed by filtration through 0.2 µm Whatman membrane filter. Carbon source

consumption and organic acids production were monitored by high pressure liquid chromatography (HPLC) using an Aminex HPX-87H (BioRad) ion exchange chromatography column, eluted at 65ºC with 5 mM H_2SO_4 at a flow rate of 0.6 ml/min for 30 min and detected by UV-Visible (UV-Vis) and refractive index (RI) detectors. Linearity of the method was tested and concentrations were estimated based on calibration curves.

Preparation of bacterial extracts and enzyme assays. Bacteria were grown in 50 ml of S medium supplemented with 2% D-glucose or D-mannitol at 37ºC for 20 hours and cells collected by centrifugation. After being washed, pellets were stored at -80ºC until used. Thawed cells were then suspended in 20 mM phosphate buffer, pH 6.8, and disrupted by sonication for 8 cycles of 30 seconds. For assays of glucose or gluconate dehydrogenases, lysates were supplemented with 1% (v/v) Triton-X100. Lysates were then centrifuged for 30 minutes at 12,000 *g*, and supernatant fractions were immediately assayed for enzyme activities.

In vitro activities of D-glucose or D-gluconate dehydrogenases (E.C. 1.1.5.2 and E.C. 1.1.99.3, respectively) were measured at 37ºC by monitoring the glucose or gluconate-dependent reduction of 0.3 mM 2,6-dichlorophenol indophenol (DCPIP) by following the decrease in absorbance of the assay mixtures at 600 nm with a spectrophotometer (UV-1700 PharmaSpec, Shimadzu). Reaction mixtures contained 150 mM phosphate buffer pH 6.8, 10 mM D-glucose (or sodium D-gluconate), 0.3 mM phenazine methosulfate (PMS), and bacterial protein extract as described previously (13). The enzyme activity was calculated using and extinction coefficient of 20600 $M^{-1}cm^{-1}$ for DCPIP. Activity of glucose-6-phosphate dehydrogenase (G6PDH) (E.C. 1.1.1.49) was determined at 37ºC by monitoring substrate-dependent formation of reduced nicotinamide adenine dinucleotide in reaction mixtures at 340

774 nm. Reaction mixtures contained 200 mM Tris.HCl pH 8.5, 0.5 mM NAD^+, 10 mM glucose-6-
775 phosphate, and bacterial protein extract. The enzyme activity was calculated using and
776 extinction coefficient of 6220 $M^{-1}cm^{-1}$ for NADH. Total activity of lactate dehydrogenase was
777 determined at 37ºC by monitoring oxidation of NADH at 340 nm in the presence of sodium
778 pyruvate. Reaction mixtures contained 50 mM 3-(N-morpholino)-propanesulfonic acid
779 (MOPS) pH 7.0, 0.12 mM NADH, 20 mM sodium pyruvate, and bacterial protein extract. One
780 unit was defined as the amount of enzyme converting 1 nmol of substrate/minute. Protein
781 concentrations were determined by using the Bradford method (BioRad reagent), using bovine
782 serum albumin as a standard protein. Enzymatic activities were performed from two biological
783 replicates and each reaction was performed five times.
784
785 **Microscopy analysis.** *B. multivorans* ATCC 17616 and the Δ*ldhR* deletion mutant
786 with/without complementation were grown up to 72 hours in S medium supplemented with D-
787 glucose or D-mannitol. Images were acquired on a commercial Leica High Content Screening
788 microscope, based on Leica DMI6000 equipped with a Hamamatsu Flash 4.0 LT sCMOS
789 camera, using a 10x 0.3 NA objective, and controlled with the Leica LAS X software (Fig. 8A,
790 Fig. S4B), or a Zeiss Axioplan equipped with a Photometrics CoolSNAP fx camera, using a
791 10x 0.3 NA objective and controlled with software MetaMorph version 4.6r9 (Fig. 8B, Fig. 9)
792 or a Pentax *ist DS digital camera (Fig. 8C, Fig. S4A). Cellular aggregate size was estimated
793 with a ruler incorporated in analysis software (Adobe Photoshop CS5) and result from at least
794 50 measures. Due to the weight of the coverslip the aggregates are flattened.
795

796 **Adhesion to surfaces and biofilm formation.** To elucidate the role of *ldhR* gene in biofilm
797 formation, cells were grown in a 24-well plate system modified from the procedure of Caiazza
798 and O´Toole (38). Briefly, overnight cultures were adjusted to an OD 600 nm of 0.1 in fresh S
799 medium supplemented with 2% D-mannitol and 100 μg/ml chloramphenicol and grown at
800 37ºC, 200 rpm in 24-well microtiter plates (Orange Scientific) at 45º angle, ensuing that the
801 air-liquid interface crossed the center of the flat-bottomed well. After 24 hours, cell cultures
802 were removed, wells washed three times with saline buffer and stained for 15 minutes with
803 crystal violet (1% solution). After washing, the extent of biofilm formation was quantified as
804 previously described (33).
805
806 ***In silico* analysis of nucleotide and amino acid sequences.** The algorithm BLAST (39)
807 was used to compare sequences of the deduced LdhR and LdhA amino acids to database
808 sequences available at the National Center for Biotechnology Information (NCBI) or the
809 Burkholderia Genome Database (http://www.burkholderia.com/bgd). Alignments were
810 performed using the program ClustalW (40). Molecular evolutionary relationships between
811 LdhA and its homologues was performed using full-length protein sequences of all 185
812 members of the D-isomer specific 2-hydroxyacid dehydrogenase family (PROSITE
813 documentation entry PDOC00063; last updated April 2006). Analyses were conducted using
814 the software package MEGA version 6.0 (41) which uses ClustalW for alignment and a
815 neighbor joining method of tree construction.
816
817 **Statistical analysis.** All quantitative data were obtained from at least three independent
818 assays with two biological replicates. Error propagation was used to calculate standard errors

and one-way analysis of variance (ANOVA) and Tukey´s multiple comparison test were performed to assess statistical significance. Differences were considered statistically significant if the *P* value was lower than 0.05.

Microarray data accession number. Microarray data were deposited in the Gene Expression Omnibus (GEO) repository at NCBI under accession numbers: GSE97006.

Ethics statement. The bacterial clinical isolates are from an anonymous patients and none of them was taken specifically for this study.

829 **ACKNOWLEDGMENTS**

830 Mário R. Santos from Instituto Gulbenkian de Ciência, Oeiras (IGC), Portugal, is
831 acknowledged for technical assistance with microscopy analysis. Microarrays were processed
832 at the IGC's Gene Expression Unit. This work was supported by Programa Operacional
833 Regional de Lisboa 2020 (LISBOA-01-0145-FEDER-007317) and Fundação para a Ciência e
834 a Tecnologia, Portugal (PTDC/QUI-BIQ/118260/2010, UID/BIO/04565/2013) and a post-
835 doctoral grant (SFRH/BPD/86475/2012) to I.N.S.

836

837 **REFERENCES**

838 1. Lipuma JJ. 2010. The changing microbial epidemiology in cystic fibrosis. Clin Microbiol
839 Rev 23:299–323.

840 2. Schwab U, Abdullah LH, Perlmutt OS, Albert D, Davis CW, Arnold RR, Yankaskas JR,
841 Gilligan P, Neubauer H, Randell SH, Boucher RC. 2014. Localization of *Burkholderia*
842 *cepacia* complex bacteria in cystic fibrosis lungs and interactions with *Pseudomonas*
843 *aeruginosa* in hypoxic mucus. Infect Immun 82:4729–4745.

844 3. Mahenthiralingam E, Urban TA, Goldberg JB. 2005. The multifarious, multireplicon
845 *Burkholderia cepacia* complex. Nat Rev Microbiol 3:144–156.

846 4. Leitão JH, Sousa SA, Ferreira AS, Ramos CG, Silva IN, Moreira LM. 2010. Pathogenicity,
847 virulence factors, and strategies to fight against *Burkholderia cepacia* complex pathogens
848 and related species. Appl Microbiol Biotechnol 87:31–40.

849 5. Ferreira AS, Silva IN, Oliveira VH, Cunha R, Moreira LM. 2011. Insights into the role of
850 extracellular polysaccharides in *Burkholderia* adaptation to different environments. Front
851 Cell Infect Microbiol 1:16.

852 6. Zlosnik JE, Hird TJ, Fraenkel MC, Moreira LM, Henry DA, Speert DP. 2008. Differential
853 mucoid exopolysaccharide production by members of the *Burkholderia cepacia* complex. J
854 Clin Microbiol 46:1470–1473.

855 7. Ferreira AS, Leitão JH, Silva IN, Pinheiro PF, Sousa SA, Ramos CG, Moreira LM. 2010.
856 Distribution of cepacian biosynthesis genes among environmental and clinical
857 *Burkholderia* strains and role of cepacian exopolysaccharide in resistance to stress
858 conditions. Appl Env Microbiol 76:441–450.

8. Cunha M V, Sousa SA, Leitão JH, Moreira LM, Videira PA, Sá-Correia I. 2004. Studies on the involvement of the exopolysaccharide produced by cystic fibrosis-associated isolates of the *Burkholderia cepacia* complex in biofilm formation and in persistence of respiratory infections. J Clin Microbiol 42:3052–3058.

9. Bylund J, Burgess LA, Cescutti P, Ernst RK, Speert DP. 2006. Exopolysaccharides from *Burkholderia cenocepacia* inhibit neutrophil chemotaxis and scavenge reactive oxygen species. J Biol Chem 281:2526–2532.

10. Conway BA, Chu KK, Bylund J, Altman E, Speert DP. 2004. Production of exopolysaccharide by *Burkholderia cenocepacia* results in altered cell-surface interactions and altered bacterial clearance in mice. J Infect Dis 190:957–966.

11. Silva IN, Tavares AC, Ferreira AS, Moreira LM. 2013. Stress conditions triggering mucoid morphotype variation in *Burkholderia* species and effect on virulence in *Galleria mellonella* and biofilm formation *in vitro*. PLoS One 8:e82522.

12. Sousa SA, Ulrich M, Bragonzi A, Burke M, Worlitzsch D, Leitão JH, Meisner C, Eberl L, Sá-Correia I, Döring G. 2007. Virulence of *Burkholderia cepacia* complex strains in gp91$^{phox-/-}$ mice. Cell Microbiol 9:2817–2825.

13. Sage A, Linker A, Evans LR, Lessie TG. 1990. Hexose phosphate metabolism and exopolysaccharide formation in *Pseudomonas cepacia*. Curr Microbiol 20:191–198.

14. Berka TR, Allenza P, Lessie TG. 1984. Hyperinduction of enzymes of the phosphorylative pathway of glucose dissimilation in *Pseudomonas cepacia*. Curr Microbiol 11:143–148.

15. Moreira LM, Videira PA, Sousa SA, Leitão JH, Cunha MV, Sá-Correia I. 2003. Identification and physical organization of the gene cluster involved in the biosynthesis of

881 *Burkholderia cepacia* complex exopolysaccharide. Biochem Biophys Res Commun
882 312:323–333.

883 16. Silva IN, Ferreira AS, Becker JD, Zlosnik JEA, Speert DP, He J, Mil-Homens D, Moreira
884 LM. 2011. Mucoid morphotype variation of *Burkholderia multivorans* during chronic
885 cystic fibrosis lung infection is correlated with changes in metabolism, motility, biofilm
886 formation and virulence. Microbiology 157:3124–3137.

887 17. Petrova OE, Schurr JR, Schurr MJ, Sauer K. 2012. Microcolony formation by the
888 opportunistic pathogen *Pseudomonas aeruginosa* requires pyruvate and pyruvate
889 fermentation. Mol Microbiol 86:819–835.

890 18. Worlitzsch D, Tarran R, Ulrich M, Schwab U, Cekici A, Meyer KC, Birrer P, Bellon G,
891 Berger J, Weiss T, Botzenhart K, Yankaskas JR, Randell S, Boucher RC, Doring G. 2002.
892 Effects of reduced mucus oxygen concentration in airway *Pseudomonas* infections of
893 cystic fibrosis patients. J Clin Invest 109:317–325.

894 19. McCarthy RR, Mooij MJ, Reen FJ, Lesouhaitier O, O'Gara F. 2014. A new regulator of
895 pathogenicity (*bvlR*) is required for full virulence and tight microcolony formation in
896 *Pseudomonas aeruginosa*. Microbiology 160:1488–1500.

897 20. Schleheck D, Barraud N, Klebensberger J, Webb JS, McDougald D, Rice SA, Kjelleberg
898 S. 2009. *Pseudomonas aeruginosa* PAO1 preferentially grows as aggregates in liquid batch
899 cultures and disperses upon starvation. PLoS One 4:e5513.

900 21. Mao D, Bushin LB, Moon K, Wu Y, Seyedsayamdost MR. 2017. Discovery of *scmR* as a
901 global regulator of secondary metabolism and virulence in *Burkholderia thailandensis*
902 E264. Proc Natl Acad Sci U S A 114:E2920–E2928.

22. Sainsbury S, Lane LA, Ren J, Gilbert RJ, Saunders NJ, Robinson CV, Stuart DI, Owens RJ. 2009. The structure of CrgA from *Neisseria meningitidis* reveals a new octameric assembly state for LysR transcriptional regulators. Nucleic Acids Res. 37:4545–4558.

23. Lessie TG, Berka T, Zamanigian S. 1979. *Pseudomonas cepacia* mutants blocked in the direct oxidative pathway of glucose degradation. J Bacteriol 139:323–325.

24. Latrach Tlemçani L, Corroler D, Barillier D, Mosrati R. 2008. Physiological states and energetic adaptation during growth of *Pseudomonas putida* mt-2 on glucose. Arch Microbiol 190:141–150.

25. de Lucena DKC, Pühler A, Weidner S. 2010. The role of sigma factor RpoH1 in the pH stress response of *Sinorhizobium meliloti*. BMC Microbiol 10:265.

26. Inhülsen S, Aguilar C, Schmid N, Suppiger A, Riedel K, Eberl L. 2012. Identification of functions linking quorum sensing with biofilm formation in *Burkholderia cenocepacia* H111. MicrobiologyOpen 1:225–242.

27. Chandler JR, Duerkop BA, Hinz A, West TE, Herman JP, Churchill MEA, Skerrett SJ, Greenberg EP. 2009. Mutational analysis of *Burkholderia thailandensis* quorum sensing and self-aggregation. J Bacteriol 191:5901–5909.

28. Kragh KN, Hutchison JB, Melaugh G, Rodesney C, Roberts AEL, Irie Y, Jensen PØ, Diggle SP, Allen RJ, Gordon V, Bjarnsholt T. 2016. Role of multicellular aggregates in biofilm formation. MBio 7:e00237-16.

29. Traverse CC, Mayo-Smith LM, Poltak SR, Cooper VS. 2013. Tangled bank of experimentally evolved *Burkholderia* biofilms reflects selection during chronic infections. Proc Natl Acad Sci U S A 110:E250-9.

925 30. Lardi M, Aguilar C, Pedrioli A, Omasits U, Suppiger A, Cárcamo-Oyarce G, Schmid N,
926 Ahrens CH, Eberl L, Pessi G. 2015. σ^{54}-dependent response to nitrogen limitation and
927 virulence in *Burkholderia cenocepacia* strain H111. Appl Environ Microbiol 81:4077–
928 4089.

929 31. Silva IN, Santos PM, Santos MR, Zlosnik JEA, Speert DP, Buskirk SW, Bruger EL,
930 Waters CM, Cooper VS, Moreira LM. 2016. Long-term evolution of *Burkholderia*
931 *multivorans* during a chronic cystic fibrosis infection reveals shifting forces of selection.
932 mSystems 1:e00029-16.

933 32. Lieberman TD, Michel J-B, Aingaran M, Potter-Bynoe G, Roux D, Davis MR, Skurnik D,
934 Leiby N, LiPuma JJ, Goldberg JB, McAdam AJ, Priebe GP, Kishony R. 2011. Parallel
935 bacterial evolution within multiple patients identifies candidate pathogenicity genes. Nat
936 Genet 43:1275–1280.

937 33. Ferreira AS, Leitão JH, Sousa SA, Cosme AM, Sá-Correia I, Moreira LM. 2007.
938 Functional analysis of *Burkholderia cepacia* genes *bceD* and *bceF*, encoding a
939 phospholyrosine phosphatase and a tyrosine autokinase, respectively: role in
940 exopolysaccharide biosynthesis and biofilm formation. Appl Environ Microbiol 73:524–
941 534.

942 34. Sambrook J, Russell DW. 2001. Molecular cloning: a laboratory manual. CSHL Press,
943 New York.

944 35. Pfaffl MW. 2001. A new mathematical model for relative quantification in real-time RT-
945 PCR. Nucleic Acids Res 29:e45.

946 36. Li C, Wong WH. 2001. Model-based analysis of oligonucleotide arrays: model validation,

947 design issues and standard error application. Genome Biol 2:RESEARCH0032.

948 37. Li C, Wong WH. 2001. Model-based analysis of oligonucleotide arrays: expression index
949 computation and outlier detection. Proc Natl Acad Sci U S A 98:31–36.

950 38. Caiazza NC, O'Toole GA. 2004. SadB is required for the transition from reversible to
951 irreversible attachment during biofilm formation by *Pseudomonas aeruginosa* PA14. J
952 Bacteriol 186:4476–4485.

953 39. Altschul SF, Madden TL, Schaffer AA, Zhang J, Zhang Z, Miller W, Lipman DJ. 1997.
954 Gapped BLAST and PSI-BLAST: a new generation of protein database search programs.
955 Nucleic Acids Res 25:3389–3402.

956 40. Thompson JD, Higgins DG, Gibson TJ. 1994. CLUSTAL W: improving the sensitivity of
957 progressive multiple sequence alignment through sequence weighting, position-specific
958 gap penalties and weight matrix choice. Nucleic Acids Res 22:4673–4680.

959 41. Tamura K, Stecher G, Peterson D, Filipski A, Kumar S. 2013. MEGA6: molecular
960 evolutionary genetics analysis Version 6.0. Mol Biol Evol 30:2725–2729.

961 42. Vandamme P, Holmes B, Vancanneyt M, Coenye T, Hoste B, Coopman R, Revets H,
962 Lauwers S, Gillis M, Kersters K, Govan JR. 1997. Occurrence of multiple genomovars of
963 *Burkholderia cepacia* in cystic fibrosis patients and proposal of *Burkholderia multivorans*
964 sp. nov. Int J Syst Bacteriol 47:1188–1200.

965 43. Mahenthiralingam E, Coenye T, Chung JW, Speert DP, Govan JR, Taylor P, Vandamme P.
966 2000. Diagnostically and experimentally useful panel of strains from the *Burkholderia*
967 *cepacia* complex. J Clin Microbiol 38:910–913.

968 44. Ferreira AS, Silva IN, Fernandes F, Pilkington R, Callaghan M, McClean S, Moreira LM.

2015. The tyrosine kinase BceF and the phosphotyrosine phosphatase BceD of *Burkholderia contaminans* are required for efficient invasion and epithelial disruption of a cystic fibrosis lung epithelial cell line. Infect Immun 83:812–821.

45. Coenye T, Vandamme P, LiPuma JJ, Govan JR, Mahenthiralingam E. 2003. Updated version of the *Burkholderia cepacia* complex experimental strain panel. J Clin Microbiol 41:2797–2798.

46. Larsen GY, Stull TL, Burns JL. 1993. Marked phenotypic variability in *Pseudomonas cepacia* isolated from a patient with cystic fibrosis. J Clin Microbiol 31:788–792.

47. Nelson MJ, Montgomery SO, O'neill EJ, Pritchard PH. 1986. Aerobic metabolism of trichloroethylene by a bacterial isolate. Appl Environ Microbiol 52:383–384.

48. LiPuma JJ, Mortensen JE, Dasen SE, Edlind TD, Schidlow D V, Burns JL, Stull TL. 1988. Ribotype analysis of *Pseudomonas cepacia* from cystic fibrosis treatment centers. J Pediatr 113:859–862.

49. Figurski DH, Helinski DR. 1979. Replication of an origin-containing derivative of plasmid RK2 dependent on a plasmid function provided in trans. Proc Natl Acad Sci U S A 76:1648–1652.

50. Sokol PA, Darling P, Woods DE, Mahenthiralingam E, Kooi C. 1999. Role of ornibactin biosynthesis in the virulence of *Burkholderia cepacia*: characterization of *pvdA*, the gene encoding L-ornithine N(5)-oxygenase. Infect Immun 67:4443–4455.

51. Vieira J, Messing J. 1991. New pUC-derived cloning vectors with different selectable markers and DNA replication origins. Gene 100:189–194.

52. Kovach ME, Phillips RW, Elzer PH, Roop 2nd RM, Peterson KM. 1994. pBBR1MCS: a

991 broad-host-range cloning vector. Biotechniques 16:800–802.

992

993 **LEGENDS**

994 **Fig. 1. Alternative pathways of gluconate-6P formation by dissimilation of glucose in**
995 ***Burkholderia***. Glucose utilization can follow the direct oxidative pathway (orange arrows) or
996 the phosphorylative pathway (blue arrows). Catabolism of other monomeric carbon sources
997 (marked with brown boxes) is also indicated. Central metabolic pathways are: glycolysis (G),
998 Entner-Doudoroff pathway (ED), pentose-phosphate pathway (PPP), tricarboxylic acid (TCA)
999 cycle, and gluconeogenesis (GN). Other abbreviations: 2KG, 2-ketogluconate; KGP, 2-
1000 ketogluconate-6P; KDPG, 2-keto-3-deoxy-gluconate-6P; *gcd*, glucose dehydrogenase; *gad*,
1001 gluconate dehydrogenase; *gntK*, glucono kinase; *kgk*, 2-ketoglucono kinase; *kgr*, KGP
1002 reductase; *zwf*, glucose-6P dehydrogenase; *glk*, glucokinase; *edd*, glucose-6P dehydratase; *eda*,
1003 KDPG aldolase; *tpi*, triose isomerase; *fba*, fructose-1,6P aldolase; *fbp*, fructose-1,6P
1004 phosphatase; *pgi*, phosphogluco isomerase; *mdh_1*, mannitol dehydrogenase; *aceA*, isocitrate
1005 lyase; *frk*, fructokinase; *ldhA*, D-lactate dehydrogenase; *phbA*, β-ketothiolase; *phbB*,
1006 acetoacetyl-CoA reductase; *phbC*, poly-β-hydroxybutyrate synthase; *gltA*, citrate synthase;
1007 *acn*, aconitate hydratase; *icdA*, isocitrate dehydrogenase; *suc*, succinate-CoA transferase; *sdh*,
1008 succinate dehydrogenase/fumarate reductase; *fum*, fumarate hydratase; *mdh*, malate
1009 dehydrogenase; *gap*, glyceraldehyde-3P dehydrogenase; *pkg*, phosphoglycerate kinase; *pgm*,
1010 phosphoglycerate mutase; *eno*, phosphopyruvate hydratase; *pta*, phosphate acetyltransferase;
1011 *ack*, acetate kinase; *pps*, phosphoenolpyruvate synthase; *pyk*, pyruvate kinase; PHB, poly-β-
1012 hydroxybutyrate; IM, inner membrane; and OM, outer membrane. This simplified catabolic
1013 pathway was based on reactions available for *B. multivorans* ATCC 17616 at Kyoto
1014 Encyclopedia of Genes and Genomes (KEGG) database.
1015

1016 **Fig. 2. The LdhR regulator shows decreased expression in nonmucoid variants derived**
1017 **from mucoid *Burkholderia* strains and is co-transcribed with gene *ldhA*.** (A) Expression by
1018 qRT-PCR of gene *ldhR* in nonmucoid variants when compared with the respective mucoid
1019 parental strains of *B. multivorans* D2095, *B. contaminans* IST408, *B. anthina* FC0967, *B.*
1020 *vietnamiensis* PC259, and *B. dolosa* CEP0743. (B) In *B. multivorans* ATCC 17616 the
1021 genomic region containing gene *ldhR* and the flanking regions are located in chromosome 1
1022 between the nucleotides position indicated in the figure. The new NCBI locus tags for the
1023 indicated genes are *BMUL_RS12975* (*Bmul_2556*), *BMUL_RS12980* (*Bmul_2557*),
1024 *BMUL_RS12985* (*Bmul_2558*), and *BMUL_RS12990* (*Bmul_2559*). Nucleotide regions
1025 upstream genes *ldhR* and *scmR* showing a *lux*-box (conserved residues in red) preceding *scmR*
1026 gene, but absent from *ldhR* upstream region. Asterisks denote conserved nucleotides between
1027 the two regions. The putative start codon is underlined. (C) Reverse transcription PCR showing
1028 the co-transcription of genes *ldhR* and *ldhA* in *B. multivorans* ATCC 17616 grown for 18 hours
1029 in S medium with 2% D-mannitol. The image shows the amplification from genomic DNA (1),
1030 cDNA (2), or total RNA (3) of the 319-bp region comprising the end of *ldhR* and beginning of
1031 *ldhA* genes; amplification from genomic DNA (4), cDNA (5), or total RNA (6) of the 305-bp
1032 region comprising the end of *ldhA* and beginning of *Bmul_2559* genes; M, DNA marker; nt,
1033 nucleotides; aa, amino acids.
1034
1035 **Fig. 3. Unrooted neighbor-joining tree of the D-isomer specific 2-hydroxyacid**
1036 **dehydrogenase superfamily (PROSITE entry PDOC00063_pattern_1.** The evolutionary
1037 history was inferred using the Neighbor-Joining method. The analysis involved 185 amino acid
1038 sequences. All positions containing gaps and missing data were eliminated. Sequences

clustering together and representing separate enzymatic subgroups are shaded. D-LDH, D-lactate dehydrogenase; SERA, D-3-phosphoglycerate dehydrogenase; PDXB, erythronate-4-phosphate dehydrogenases; FDH, formate dehydrogenase; GHPR, glyoxylate/hydroxypyruvate reductases; and CTBP, C-terminal binding protein. *B. multivorans* LdhA is in red color.

Fig. 4. LdhR decreases exopolysaccharide production. (A) Production of EPS by the WT *B. multivorans* ATCC 17616 (WT) and the Δ*ldhR* mutant in the presence of different sugars as main carbon source for 3 days at 37ºC. EPS production is expressed as ethanol precipitate dry weight (g/l). Significantly greater amount of EPS was produced by the Δ*ldhR* mutant (*, $P<0.05$; **, $P<0.01$; ***, $P<0.001$), by Tukey´s HSD multiple comparison test. (B) Effect on EPS production by the complementation of the wild-type strain or the Δ*ldhR* mutant by expressing *in trans* the *ldhRA* genes from pARG015-1 or the empty vector pBBR1MCS. Cells were incubated in the presence of the indicated sugars for 3 days at 37ºC followed by EPS quantification. Significantly lower amount of EPS was produced when the *ldhRA* genes were overexpressed in both WT and mutant strain (*, $P<0.05$; **, $P<0.01$; ***, $P<0.001$), by Tukey´s HSD multiple comparison test.

Fig. 5. Loss of cell viability and medium acidification is dependent on the glucose concentration. Culture growth as measured by turbidity (OD_{640nm}) and colony forming units (CFU) plating of *B. multivorans* ATCC 17616 and the Δ*ldhR* mutant grown for 72 hours in the presence of 2% of D-mannitol (A) and 0.5 or 2% D-glucose (B, C). Culture medium pH in the presence of D-glucose is shown in panel D. Error bars indicate the standard deviation.

1062 **Fig. 6. Complementation of the Δ*ldhR* mutant only rescues the wild-type growth**
1063 **properties in glucose-rich medium if gene *ldhA* is expressed alone or together with *ldhR*.**
1064 Culture growth as measured by turbidity (OD_{640nm}) (A) and colony forming units (B) of Δ*ldhR*
1065 mutant complemented with empty vector pBBR1MCS, pMM137-2 expressing *ldhR* gene from
1066 the bce promoter, pLM016-2 expressing *ldhA* gene from the bce promoter, and pARG015-1
1067 expressing *ldhRA* genes from their own promoter. (C) Culture medium pH measured for the
1068 indicated strains. Genotype symbols are consistent for each panel. Cells were grown in
1069 medium supplemented with 2% D-glucose. (D) Quantitative RT-PCR analysis of transcript
1070 levels of genes *ldhR* and *ldhA* in the WT *B. multivorans* ATCC 17616, Δ*ldhR* mutant, and
1071 Δ*ldhR* mutant expressing *ldhR* gene from pMM137-2. Cells were grown in medium
1072 supplemented with D-glucose for 22 hours at 37ºC. Error bars indicate standard deviation.
1073
1074 **Fig. 7. D-lactate accumulation in the culture medium was only observed for the wild-type**
1075 **strain.** Concentration of the organic acids gluconate (GN) and 2-ketogluconate (2KG) (A), and
1076 D-lactate (B, right scale) in the supernatants of *B. multivorans* ATCC 17616 wild-type cells
1077 and the Δ*ldhR* mutant in medium supplemented with 2% D-glucose as measured by HPLC.
1078 Glucose consumption is shown in panel B (left scale). (C) Levels of the enzymes glucose
1079 dehydrogenase (GDH), gluconate dehydrogenase (GNDH), glucose-6P dehydrogenase
1080 (G6PDH) and lactate dehydrogenase (LDH) in total extracts of the indicated strains grown for
1081 20 hours in S medium supplemented with 2% D-glucose, or 2% D-mannitol. Significantly
1082 lower enzymatic activity was found for the *ldhRA* mutant when compared to the WT strain (**,
1083 $P<0.01$; ***, $P<0.001$), by Tukey´s HSD multiple comparison test. (D) Sugar consumption at
1084 48 hours of growth by *B. multivorans* ATCC 17616 cells and the Δ*ldhR* mutant in medium

supplemented with 2% (111 mM) D-sugar as measured by HPLC. Glc, D-glucose; Gal, D-galactose; Fru, D-fructose; Man, D-mannose. Error bars indicate the standard deviation.

Fig. 8. Planktonic cellular aggregates development and biofilm formation is dependent on LdhR and LdhA activities. (A) Images of planktonic aggregates formed during growth of *B. multivorans* ATCC 17616 wild-type cells and the Δ*ldhR* deletion mutant in medium supplemented with 2% D-mannitol for the indicated times. (B) Images of the planktonic cellular aggregates that sediment after 5 minutes static incubation of the indicated cultures grown for 72 hours under constant agitation in medium containing 2% D-mannitol. The bar scale is shown. (C) Images of biofilm cells attached to the solid surface of 24-well microtiter plates after 24 hours of incubation with agitation in medium containing 2% D-mannitol and biofilm quantification by the crystal violet staining method. The bar scale of images from panel C measures 2.5 mm.

Fig. 9. Planktonic growth of several strains from the *B. cepacia* complex leads to cellular aggregate formation. Phase contrast microscopy images of planktonic cellular aggregates obtained after 3 days of liquid batch cultures grown in medium supplemented with 2% D-mannitol (left panel) for the indicated strains. Bar scale shown in panel Q is the same for all other images. Right panel bottom shows the number of isolates of each *B. cepacia* complex species analyzed and their ability to form planktonic cellular aggregates. UTI, urinary tract infection; CF, cystic fibrosis infection; and CGD, chronic granulomatous disease.

1107 **Table 1** Acidification of the culture medium and secretion and consumption of D-lactate as a

1108 consequence of 2% D-glucose dissimilation.

Strain	Characteristics	Medium acidification/ maximal recovery (pH)	D-lactate secretion/ consumption
B. multivorans JTC	Chronic granulomatous disease	4.0/6.3	yes/yes
B. multivorans VC3161	Cystic fibrosis isolate	3.6/3.6	yes/no
B. multivorans VC7495	Cystic fibrosis isolate	4.0/6.5	yes/yes
B. multivorans VC6882	Cystic fibrosis isolate	4.9/6.3	yes/yes
B. multivorans VC12539	Cystic fibrosis isolate	4.8/6.6	yes/yes
B. multivorans VC8086	Cystic fibrosis isolate	4.8/6.6	yes/yes
B. multivorans VC9159	Cystic fibrosis isolate	4.0/6.4	yes/yes
B. multivorans VC12675	Cystic fibrosis isolate	4.9/6.2	yes/yes
B. multivorans D2095	Cystic fibrosis isolate	3.5/3.5	yes/no
B. ambifaria CEP0996	Cystic fibrosis isolate	5.1/6.7	yes/yes
B. stabilis LMG 14294	Cystic fibrosis isolate	6.1/6.7	yes/yes
B. anthina J2552	Rhizosphere	5.2/6.9	n.d./ n.a.
B. dolosa CEP1010	Cystic fibrosis isolate	3.7/3.7	yes/no
B. cenocepacia ATCC 17765	Urinary tract infection	6.3/7.1	yes/yes
B. cenocepacia J2315	Cystic fibrosis isolate	6.5/6.5	n.d./ n.a.
B. cepacia ATCC 25416	*Allium cepa*	5.7/7.0	n.d./ n.a.
B. contaminans IST408	Cystic fibrosis isolate	4.5/5.9	n.d./n.a.
B. vietnamiensis G4	Industrial waste treatment facility	5.5/6.3	n.d./n.a.

1109 n.d., not detected; n.a., not applicable.

1110

1111 **Table 2** Selection of a set of differentially expressed genes, separated by functional groups,

1112 when the Δ*ldhR* mutant transcriptome was compared with the one of *B. multivorans* ATCC

1113 17616, obtained in medium supplemented with 2% D-glucose.

Functional class	Gene identifier	LB-FC[a]	Gene name	Description
Regulatory genes				
	Bmul_0486	-1.3	*rpoH*	RNA polymerase factor sigma-32
	Bmul_1123	1.3	*glnL*	signal transduction histidine kinase, N_2 specific, NtrB
	Bmul_1722	-1.3	*hfq2*	RNA chaperone Hfq
	Bmul_2393	-1.3	-	cold-shock DNA-binding domain-containing protein
	Bmul_2400	-1.2	*rpoZ*	DNA-directed RNA polymerase, omega subunit
Nitrogen acquisition and assimilation				
	Bmul_0437	2.4	*glnB-1*	nitrogen regulatory protein P-II

	Bmul_0438	1.4	*amt*	ammonium transporter
	Bmul_1122	1.8	*glnA*	glutamine synthetase, type I
	Bmul_1636	-1.4	*sbp*	ABC transporter periplasmic sulfate-binding protein
	Bmul_2482	1.4	*urtA*	urea ABC transporter urea binding protein
	Bmul_4146	1.3	*narK*	major facilitator superfamily MFS_1
	Bmul_4147	1.7	*nirB*	nitrite reductase (NAD(P)H), large subunit
	Bmul_4148	2.0	*nirD*	nitrite reductase (NAD(P)H), small subunit
	Bmul_4149	1.3	*nos*	molybdopterin oxidoreductase
Carbon metabolism and energy production				
	Bmul_2649	-1.9	-	oxidoreductase FAD/NAD(P)-binding domain protein
	Bmul_3307	-1.4	*cydA*	cytochrome bd ubiquinol oxidase subunit I
	Bmul_3795	2.2	-	TonB-dependent siderophore receptor
	Bmul_5321	-1.7	-	2-amino-3-ketobutyrate coenzyme A ligase
Posttranslational modification, protein turnover, chaperones				
	Bmul_0546	-1.2	-	peptidase M48 Ste24p
	Bmul_0776	-1.3	*clpS*	ATP-dependent Clp protease adaptor protein ClpS
	Bmul_1348	-1.2	*tig*	trigger factor
	Bmul_1351	-1.3	*lon*	ATP-dependent protease La
	Bmul_1426	-1.3	*clpB*	ATP-dependent chaperone ClpB
	Bmul_2055	-1.5	-	heat shock protein Hsp20
	Bmul_2056	-1.3	-	heat shock protein Hsp20
	Bmul_2384	-1.4	-	heat shock protein Hsp20
	Bmul_2528	-1.5	*groEL*	chaperonin GroEL
	Bmul_2529	-1.6	*groES*	chaperonin Cpn10
	Bmul_2633	-1.7	*dnaK*	chaperone protein DnaK
	Bmul_2635	-1.4	*grpE*	heat shock protein GrpE
	Bmul_3087	-1.3	*hslU*	ATP-dependent protease ATP-binding subunit HslU
Secondary metabolism				
	Bmul_5943	-1.4	-	deoxyxylulose-5P synthase
	Bmul_5944	-1.4	-	methyltransferase type 12
	Bmul_5945	-1.5	-	methyltransferase type 12
	Bmul_5946	-1.6	-	Rieske (2Fe-2S) domain containing protein
	Bmul_5947	-1.5	-	hypothetical protein
	Bmul_5948	-1.4	-	cytochrome P450
	Bmul_5949	-1.4	-	Rieske (2Fe-2S) domain containing protein

[a], LB-FC, lower bound of fold change.

1118 **Table 3** Strains and plasmids used in this work.

Strain and plasmid*	Relevant characteristic	Source/ reference
Strains		
B. multivorans ATCC 17616	Soil isolate, USA; EPS^+	(42)
B. multivorans Δ*ldhR*	ATCC 17616-derivative with the *ldhR* gene replaced by a trimethoprim resistance cassette	This work
B. multivorans D2095	Cystic fibrosis isolate, Canada; EPS^+	(16)
B. multivorans D2095-nmv	Nonmucoid variant obtained under nutrient starvation; EPS^-	(11)
B. multivorans VC5602	Cystic fibrosis isolate, Canada; EPS^+	(31)
B. multivorans VC5602-nmv1	VC5602-derivative with a frameshift mutation in *bceF* gene, EPS^-	Moreira LM (unpublished)
B. multivorans CF-A1-1	Cystic fibrosis isolate, Canada	D. P. Speert
B. multivorans VC9159	Cystic fibrosis isolate, Canada	D. P. Speert
B. multivorans VC8086	Cystic fibrosis isolate, Canada	D. P. Speert
B. multivorans VC10037	Cystic fibrosis isolate, Canada	D. P. Speert
B. multivorans JTC	Chronic granulomatous disease, USA	(43)
B. multivorans VC3161	Cystic fibrosis isolate, Canada	D. P. Speert
B. multivorans VC7495	Cystic fibrosis isolate, Canada	D. P. Speert
B. multivorans VC6882	Cystic fibrosis isolate, Canada	D. P. Speert
B. multivorans VC12539	Cystic fibrosis isolate, Canada	D. P. Speert
B. multivorans VC12675	Cystic fibrosis isolate, Canada	D. P. Speert
B. contaminans IST408	Cystic fibrosis isolate, Portugal; EPS^+	(44)
B. contaminans IST408-nmv	Nonmucoid variant obtained under nutrient starvation; EPS^-	(11)
B. contaminans strain E	Cystic fibrosis isolate, Argentina	J. Degrossi
B. anthina FC0967	Cystic fibrosis isolate, Canada; EPS^+	D. P. Speert
B. anthina FC0967-nmv	Nonmucoid variant obtained under nutrient starvation; EPS^-	(11)
B. anthina J2552	Rhizosphere, UK	(45)
B. vietnamiensis PC259	Cystic fibrosis isolate, USA; EPS^+	(46)
B. vietnamiensis PC259-nmv	Nonmucoid variant obtained under nutrient starvation; EPS^-	(11)
B. vietnamiensis FC0441	Chronic granulomatous disease , Canada	D. P. Speert
B. vietnamiensis G4	Industrial waste treatment facility, USA	(47)
B. dolosa CEP0743	Cystic fibrosis isolate, Canada; EPS^+	D. P. Speert
B. dolosa CEP0743-nmv	Nonmucoid variant obtained under nutrient starvation; EPS^-	(11)
B. dolosa CEP0021	Cystic fibrosis isolate, Canada	D. P. Speert
B. dolosa CEP1010	Cystic fibrosis isolate, Canada	D. P. Speert
B. cepacia LMG 17997	Urinary tract infection, Sweden	(43)
B. cepacia FC1101	Cystic fibrosis isolate, Canada	D. P. Speert
B. cepacia ATCC 25416	Allium cepa, USA	(43)
B. cenocepacia PC184	Cystic fibrosis isolate, USA	(48)
B. cenocepacia CEP0571	Cystic fibrosis isolate, Canada	D. P. Speert
B. cenocepacia FC0447	Cystic fibrosis isolate, Canada	D. P. Speert
B. cenocepacia ATCC 17765	Urinary tract infection, UK	(43)
B. cenocepacia J2315	Cystic fibrosis isolate, UK	(43)
B. stabilis C7322	Cystic fibrosis isolate, Canada	D. P. Speert
B. stabilis LMG 14294	Cystic fibrosis isolate, Belgium	(43)

B. ambifaria FC0168	Cystic fibrosis isolate, Canada	D. P. Speert
B. ambifaria CEP0958	Cystic fibrosis isolate, Canada	D. P. Speert
B. ambifaria CEP0996	Cystic fibrosis isolate, Australia	(45)
P. aeruginosa FC1061	Cystic fibrosis isolate, Canada	D. P. Speert
P. aeruginosa 005	Cystic fibrosis isolate, Canada	D. P. Speert
Escherichia coli DH5α	DH5α *recA1*, *lac*Ui69, o80d*lac*Z ΔM15	Gibco BRL
Plasmids		
pRK2013	Tra^+ Mob^+ (RK2) Km::*Tn7* ColE1 origin, helper plasmid, Km^r	(49)
pBCKS	3.4-kb phagemid derived from pUC19; *lac* promoter, Cm^r	Stratagene
pUC-TP	pUC-GM derivative with a 1.1-kb Tp^r gene cassette, Ap^r Tp^r	(50)
pUK21	3089-bp pUC21 derivative, Km^r	(51)
pBBR1MCS	4,717-bp broad-host-range cloning vector, Cm^r	(52)
pAT312	pBCKS derivative containing the 1719-bp HindIII/XbaI fragment upstream of *ldhR* gene	This work
pAT812	pAT312 derivative containing the 1800-bp XbaI/SacI fragment downstream of *ldhR* gene	This work
pAT812-Tp	pAT812 derivative containing the trimethoprim resistance cassette	This work
pLM135-5	pUK21 derivative containing a 0.4-kb HindIII/NdeI fragment with the *bce* genes promoter region	(44)
pMM137-1	pLM135-5 derivative containing a 1070-bp NdeI/XbaI fragment with the *ldhR* gene	This work
pLM016-1	pLM135-5 derivative containing a 1002-bp NdeI/XbaI fragment with the *ldhA* gene	This work
pMM137-2	pBBR1MCS derivative containing the bce promoter and *ldhR* gene from pLM137-1	This work
pLM016-2	pBBR1MCS derivative containing the bce promoter and *ldhA* gene from pLM016-1	This work
pARG015-1	pBBR1MCS derivative containing a HindIII fragment expressing the *ldhRA* gene from their own promoter	This work

Abbreviations: Tp^r, trimethoprim resistance; Cm^r, chloramphenicol resistance; Km^r, kanamycin resistance; Ap^r, ampicillin resistance; EPS^+, exopolysaccharide producer; *Due to the high number of strains tested in Figure 9, only the ones forming planktonic cellular aggregates were here included.

1128 **Table 4** List of primers used in this work.

Gene region	Forward*	Reverse*
Bmul2557L	GAA*TCTAGA*CATGGTCTGAATCTGG	CCT*AAGCTT*GCTTCGAGATATGGC
Bmul2557R	AGC*GAGCTC*GTTCGAGCATCGGCTT	GAC*TCTAGA*CCGGGCCTGCAGTAAA
P1	GCAA*CATATG*AACCAGATTCAGACCATG	TTG*TCTAGA*GTGAACGAATCGTCGTCGTA
P2	CATG*CATATG*CGCGTGATCCTGTTCAGC	CG*TCTAGA*GGCGTATCAGCGGCTC
P3	GCG*AAGCTT*GCGCGCGGATTGTG	AGG*AAGCTT*GCGGAAGGCCGAAG
2557/2558_RT	TCGAACATGCGATCGAGCACTT	TCGAGCGTGTCGTTGACGAA
2558/2559_RT	CTCGCGAACATCGAAGCGT	CGACGTGAAATGGCGCATGT
qRT_2557	CACTCGTCACGCGTTCGAT	GGTGGATCAGCCGCGTAT
qRT_2558	CGTGTTCGCGAAGATCATGA	TACGGCGGCATCGAATG
qRT_trpB	GACTGGGTCACGAACATCGAGAA	ACACCGAATGCGTCTCGATGA

1129 *, restriction sites are in italics.

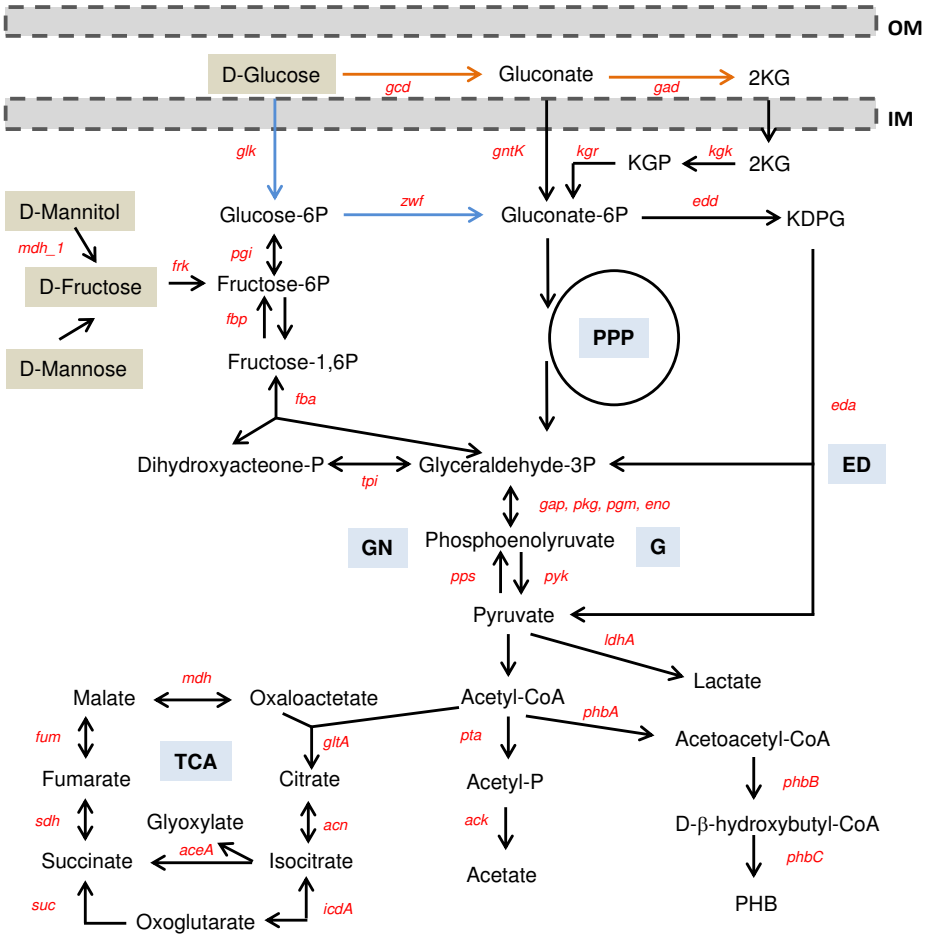

Fig. 1

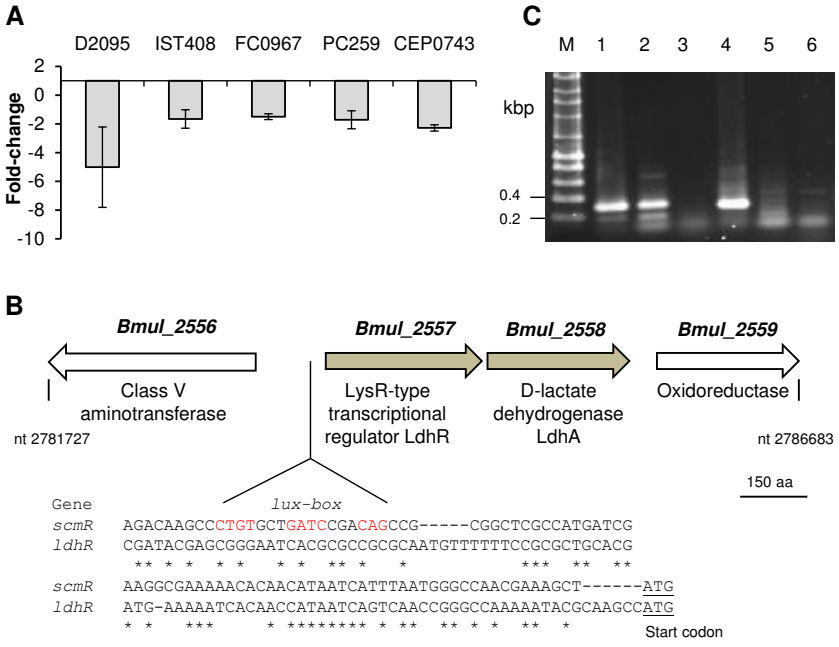

Fig. 2

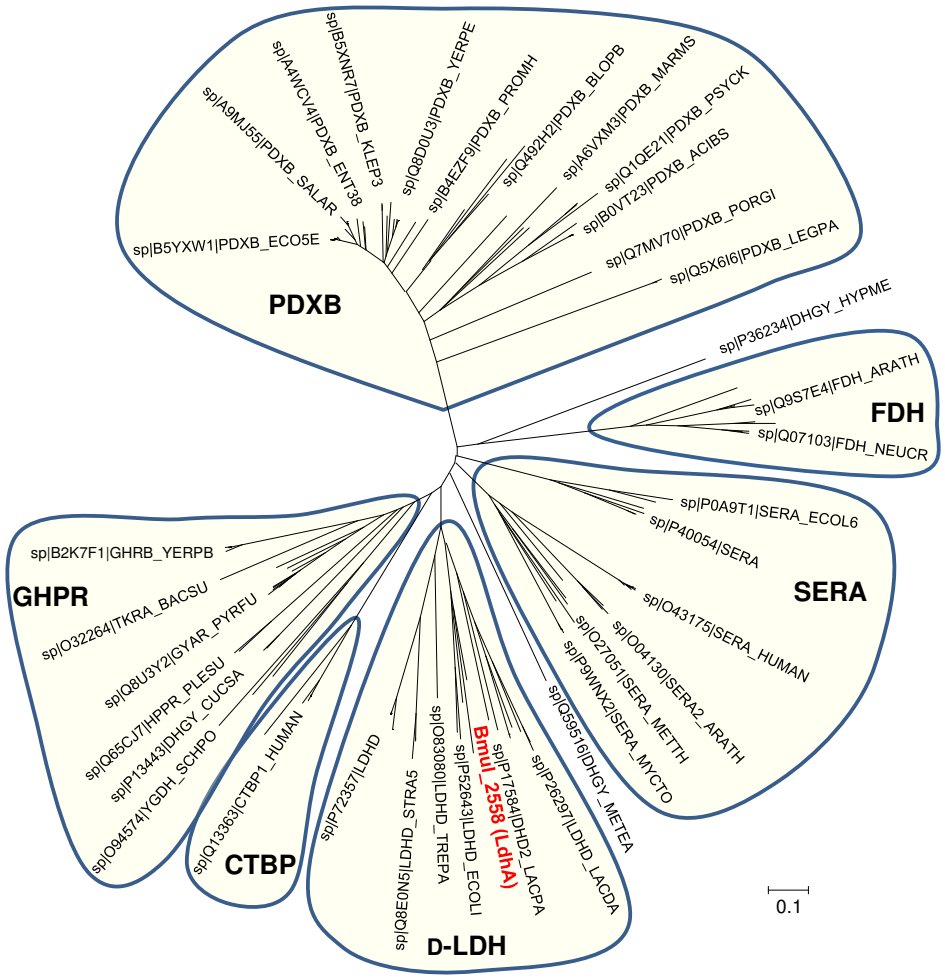

Fig. 3

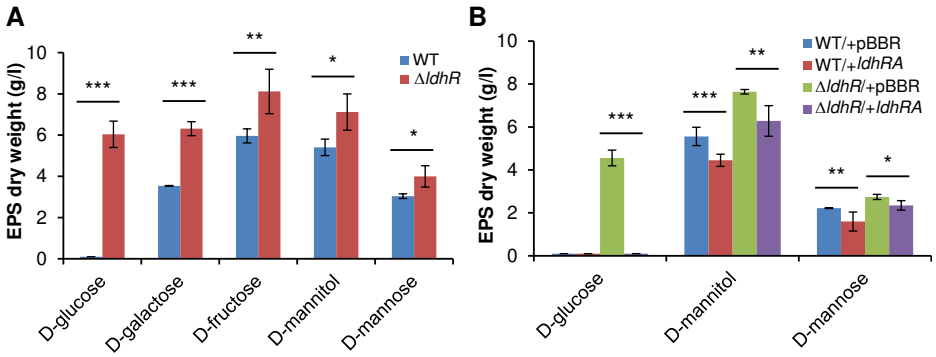

Fig. 4

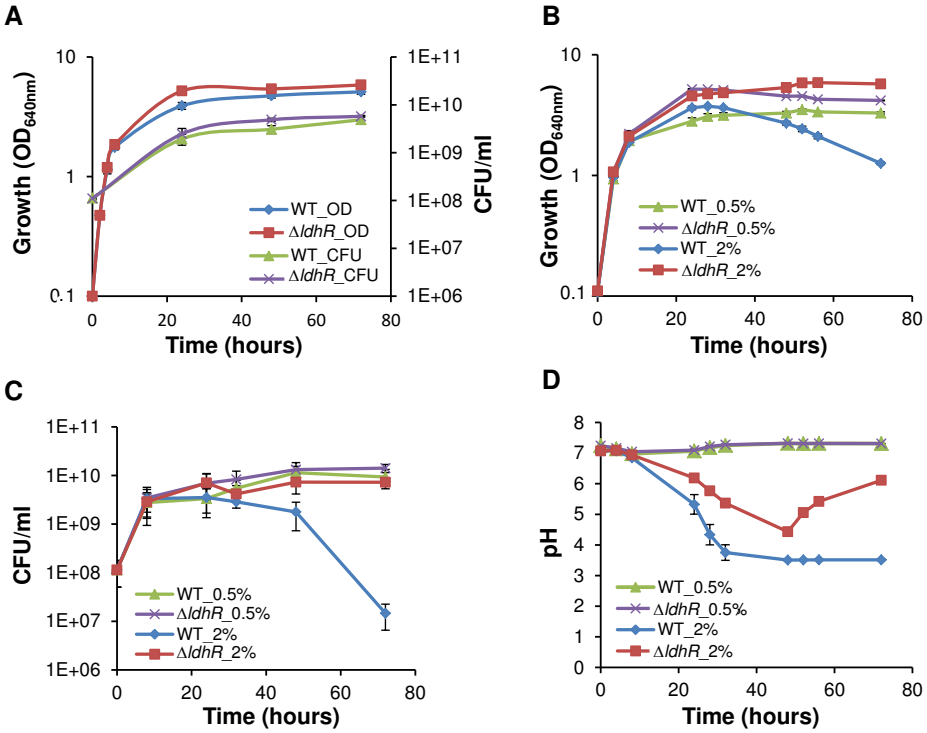

Fig. 5

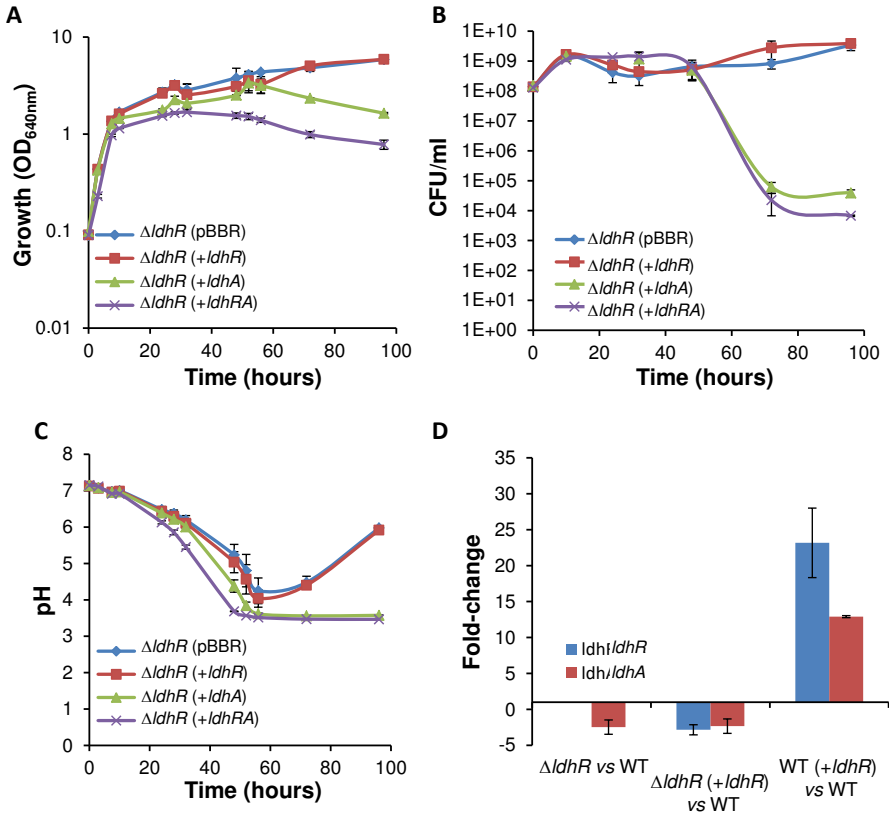

Fig. 6

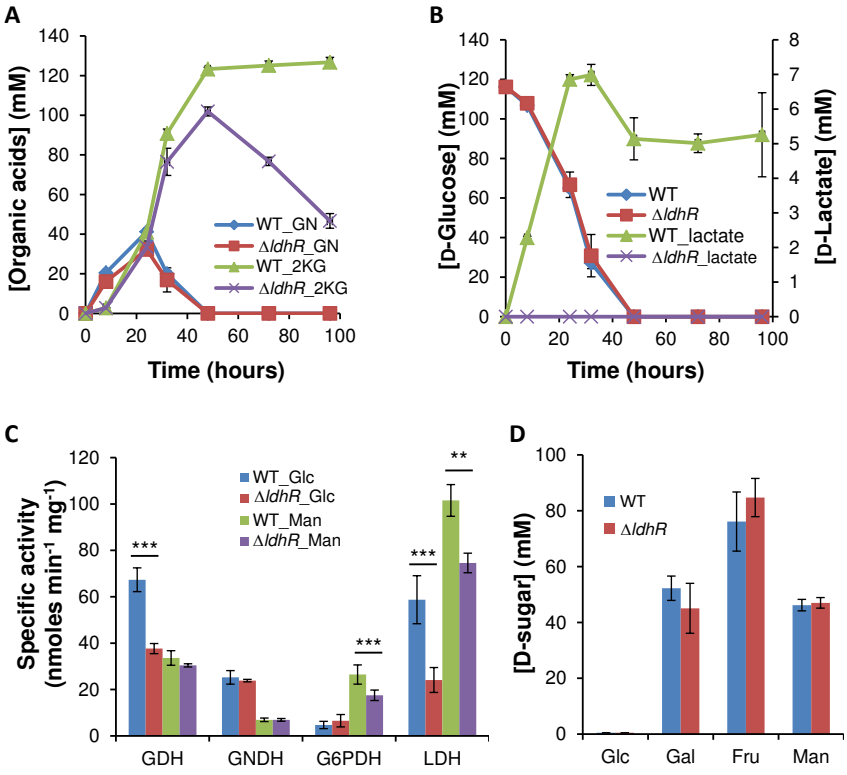

Fig. 7

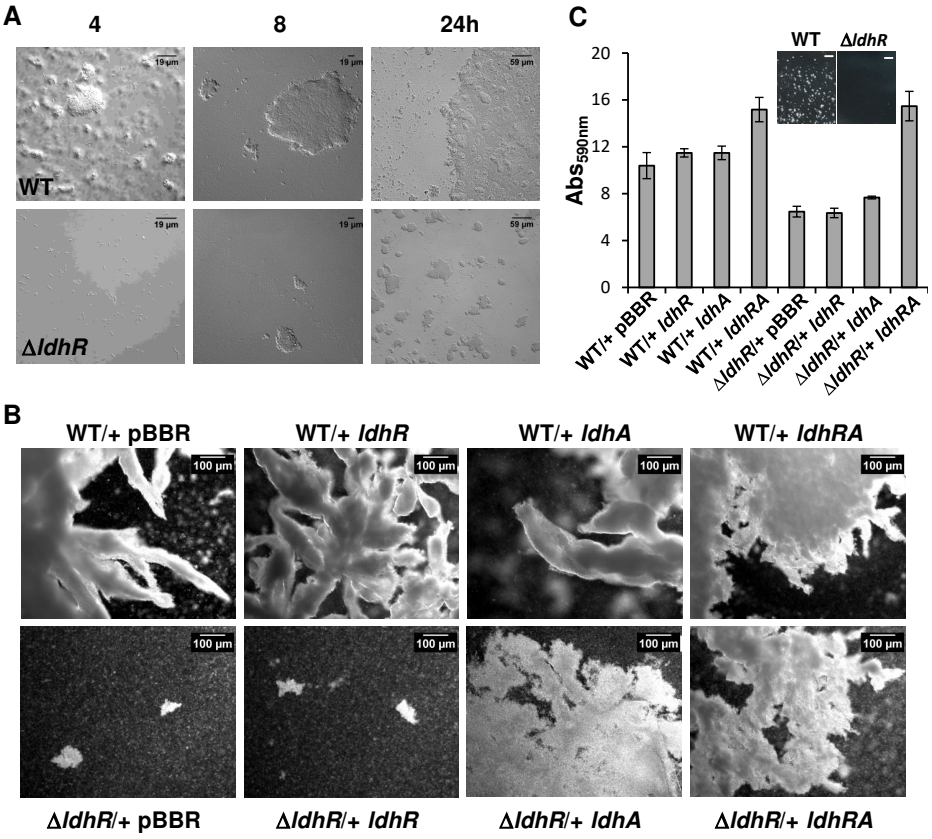

Fig. 8

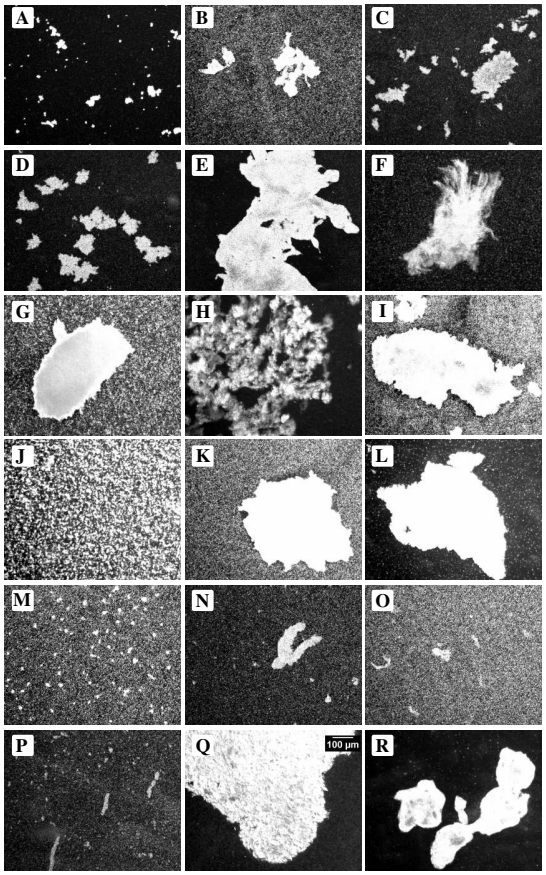

A- *B. cepacia* LMG 17997 UTI
B- *B. cepacia* FC1101 CF
C- *B. multivorans* CF-A1-1 CF
D- *B. multivorans* VC9159 CF
E- *B. multivorans* VC8086 CF
F- *B. multivorans* VC10037 CF
G- *B. cenocepacia* PC184 CF
H- *B. cenocepacia* CEP0571 CF
I- *B. cenocepacia* FC0447 CF
J- *B. stabilis* C7322 CF
K- *B. dolosa* CEP0021 CF
L- *B. vietnamiensis* FC0441 CGD
M- *B. contaminans* IST408 CF
N- *B. contaminans* strain E CF
O- *B. ambifaria* FC0168 CF
P- *B. ambifaria* CEP0958 CF
Q- *P. aeruginosa* FC1061 CF
R- *P. aeruginosa* 005 CF

***Burkholderia* species**	**With aggregates**	**Without aggregates**
B. cepacia	3	4
B. multivorans	14	3
B. cenocepacia	8	6
B. stabilis	1	3
B. vietnamiensis	1	5
B. dolosa	1	4
B. ambifaria	4	1
B. anthina	0	4
B. contaminans	8	4

Fig. 9